Journal Pre-proofs

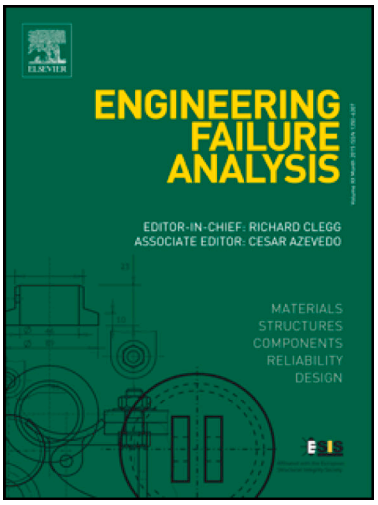

Seismic vulnerability assessment and earthquake response of slender historical masonry bell towers in South-East Lombardia

Marco Valente

PII: S1350-6307(21)00517-3
DOI: https://doi.org/10.1016/j.engfailanal.2021.105656
Reference: EFA 105656

To appear in: *Engineering Failure Analysis*

Received Date: 18 March 2021
Revised Date: 29 July 2021
Accepted Date: 30 July 2021

Please cite this article as: Valente, M., Seismic vulnerability assessment and earthquake response of slender historical masonry bell towers in South-East Lombardia, *Engineering Failure Analysis* (2021), doi: https://doi.org/10.1016/j.engfailanal.2021.105656

Seismic vulnerability assessment and earthquake response of slender historical masonry bell towers in South-East Lombardia

by
Marco VALENTE*(1)

(1) Department of Architecture, Built Environment and Construction Engineering
Politecnico di Milano, Milano, Italy
** Corresponding author. E-mail: marco.valente@polimi.it.*
Phone: +39 022399 4266 Fax: +39 022399 4220

Abstract

Masonry bell towers represent a large portion of the Italian cultural heritage and are highly vulnerable to seismic actions mainly due to their relevant slenderness, as also observed in recent seismic events. The present study investigates the seismic vulnerability and earthquake response of five slender historical masonry bell towers, which are located in South-East Lombardia (Northern Italy), through a preliminary simplified procedure suggested by the Italian Code and advanced numerical simulations. To thoroughly study the seismic response of the bell towers, detailed three-dimensional FE models with a damage plasticity constitutive law for masonry are developed and non-linear dynamic analyses are performed using different accelerograms. The results of the non-linear dynamic analyses show that the geometrical features and the main vibration properties of the bell towers turn out to be the main parameters influencing the seismic performance of such a construction typology. Moreover, it can be noted a clear influence of the accelerograms characteristics on both the energy dissipated by tensile damage and the maximum normalized displacements of the bell towers. On the other hand, the structural geometrical characteristics play a very important role in terms of damage distribution among the different parts of the bell towers. In addition, the main limitations of the simplified approach suggested by the Italian Code for the seismic assessment of the bell towers under study are highlighted through a comparison with the results obtained from non-linear dynamic analyses. The main outcomes presented in this study may also represent a useful insight to better understand the earthquake response and seismic vulnerability of similar masonry bell towers located in the same region, providing valuable information that can be directly used in seismic risk assessment at regional scale.

Keywords: masonry bell tower; seismic assessment; simplified procedure; non-linear dynamic analysis; damage distribution.

1. Introduction

The seismic vulnerability assessment of masonry constructions belonging to architectural heritage and their preservation against lateral loads are still a critical issue and represent a current challenging research topic [1-6]. The experience of past seismic events has highlighted that earthquakes of small-to-moderate intensity can cause severe damage and even collapse of such a typology of structures [7-14]. In particular, historical masonry towers can be considered highly vulnerable to horizontal loads due to their high slenderness combined with the presence of severe irregularities, large openings, leaning phenomena, heterogeneity and very low tensile strength of masonry: a proper prediction of the seismic response and damage distribution of historical masonry towers and minarets still represent a complex task [15-36].

This paper presents a numerical study on the seismic vulnerability assessment and earthquake response evaluation of five slender ancient masonry bell towers that are representative of a structural typology very common in South-East Lombardia, Northern Italy.

The seismic safety evaluation of the bell towers has been carried out, in a preliminary phase, using a procedure based on a simplified mechanical based approach in order to assess a seismic safety index in terms of peak ground acceleration. The synthetic theoretical predictions obtained through the simplified procedure have been summarized for all the case studies, providing a preliminary indication of the seismic vulnerability of the bell towers that can be effectively used at territorial scale. In a second phase, the critical issues related to the application of the simplified procedure for the seismic assessment of the bell towers have been highlighted through a comparison with the results obtained through non-linear dynamic analyses.

For the advanced numerical simulations, a detailed three-dimensional FE model with a damage plasticity constitutive law for masonry has been developed for each bell tower and non-linear dynamic analyses have been performed. The same masonry material has been assumed for all the bell towers in order to have an insight into the seismic behavior of the structures only as a function of their geometry. The seismic response of the bell towers has been evaluated in terms of maximum normalized displacements, damage distribution and energy density dissipated by tensile damage. The geometrical features and the main vibration properties turn out to be the main parameters influencing the seismic structural performance of the bell towers.

Some of the main objectives of this study can be summarized as outlined below: (1) to identify the most vulnerable parts of the bell towers under study, which are representative of a structural typology very widespread in South-East Lombardia; (2) to obtain a thorough understanding of the seismic response and damage distribution of the bell towers through the analysis of important response parameters for different PGA levels and different accelerograms; (3) to highlight the main limitations of the simplified procedure through a comparison with the results obtained from non-linear dynamic analyses. The main findings of this study may contribute to a better understanding of the seismic vulnerability of this typology of masonry constructions, providing useful information that can be directly used in seismic risk assessment at regional scale.

The paper is organized as follows. Section 2 provides a concise description of the five case studies. Section 3 presents the main results of a preliminary seismic vulnerability assessment of the bell towers using the simplified mechanical based approach suggested by the Italian Code. Section 4 describes the FE models and the material constitutive law used for masonry in the advanced numerical simulations: in addition, a preliminary evaluation of the dynamic behavior of the five bell towers through modal analysis is provided. Section 5 illustrates the main results of the non-linear dynamic analyses performed on the detailed FE models of the bell towers and a comparative discussion of the main outcomes obtained in this study is presented in Section 6. Finally, the main conclusions of this research are reported in Section 7.

2. Description of the towers under study

This section provides a short description of the five bell towers under study, which are schematically illustrated in Fig. 1. It can be noted that the geometrical characteristics of the bell towers are quite similar, because the case studies represent a typical structural typology that can be commonly observed in the South-East of Lombardia, Northern Italy. Moreover, it is reasonable to consider that the five bell towers are characterized by a similar masonry because they were built in the same geographical area and approximately in the same period.

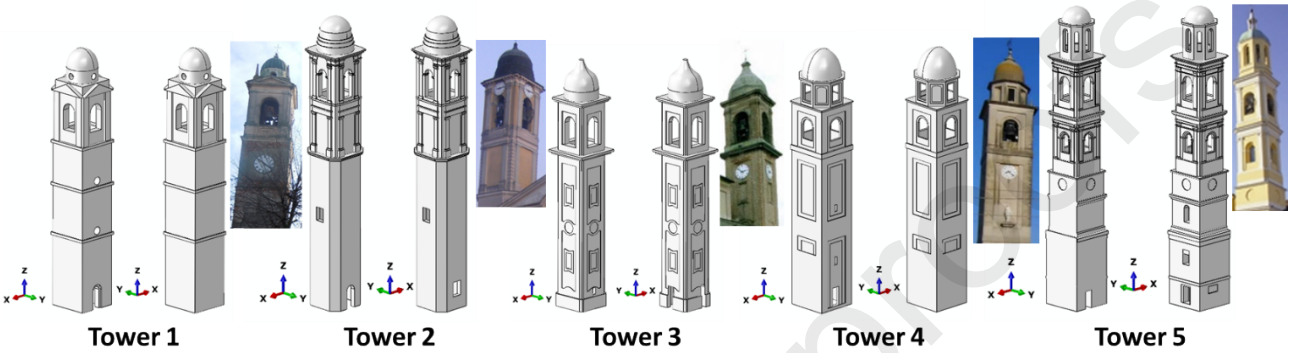

Fig 1. Schematic three-dimensional views and photos of the five bell towers under study.

2.1. Tower 1

The bell tower, which is about 29 m high, is characterized by a square plan with sides equal to about 4.5 m. The walls thickness remains constant along the height until about 18.7 m and is equal to around 1 m for all the four sides. A small dome with a diameter of about 3.5 m is present on the top of the bell tower. The bottom part of the bell tower, up to a height of about 20 m, is almost devoid of any openings; only the east side presents the entrance door at the base and two small circular openings at mid-height. In the upper part, each side exhibits a large arched opening that is about 3.1 m high. The bell tower is characterized by the presence of decorative cornices at regular intervals, pilasters on both sides of the belfry openings and triangular tympanums protruding above them.
Fig. 2 shows the elevation views of the four sides of Tower 1 along with the sections at relevant different heights with indications of the main geometrical dimensions.

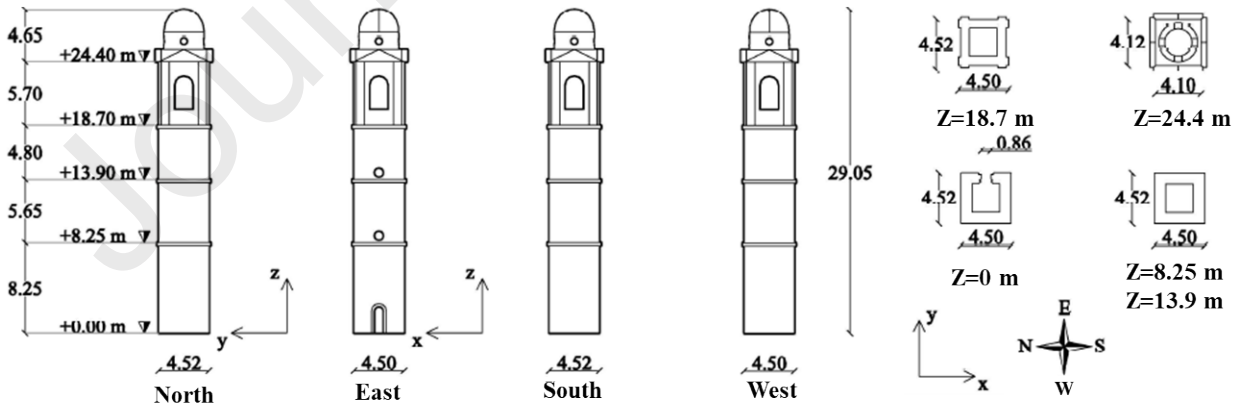

Fig. 2. Tower 1. Elevation views, plan and relevant sections of the bell tower with indication of the main geometrical dimensions.

2.2. Tower 2

The bell tower, which is about 34 m high, is characterized by an approximately octagonal plan in the lower part (up to a height of about 18 m) and by a square section in the upper part. The length of the

external sides including the section at the base is equal to 4.8 m, while the square section in the upper part presents a side equal to 4 m. The walls thickness remains constant along the height: in the lower part it is equal to 0.5 m for the four main sides and 0.9 m for the diagonal ones, while in the upper part (square section) it is equal to 0.5 m. A small dome, which exhibits a diameter of about 3.6 m, is present on the top of the bell tower: it is supported by a circular tambour consisting of different layers that are characterized by a thickness decreasing with the height.
In the lower part of the bell tower, a small opening, which is 1.6 m high, is present on two parallel sides. The entrance door, which is 2.7 m high, is present on the north side: a window, which is 1.7 m high, can be found on the south side at the ground level. The belfry presents a large arched opening, which is 3.4 m high, on each side.
The upper part of the bell tower is characterized by many decorations, such as cornices at regular intervals, the first of which separates the octagonal section from the square one. Moreover, in the upper part two rows of pilasters are present on each side, enclosing also the belfry openings.
Fig. 3 shows the elevation views of the four sides of Tower 2 along with the sections at relevant different heights with indications of the main geometrical dimensions.

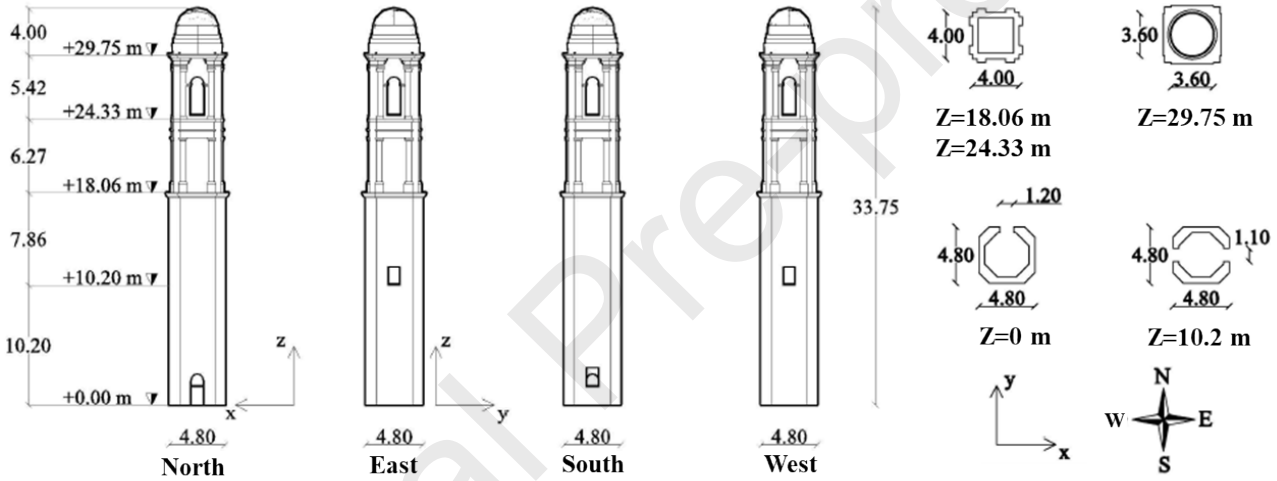

Fig. 3. Tower 2. Elevation views, plan and relevant sections of the bell tower with indication of the main geometrical dimensions.

2.3. Tower 3

The bell tower, which is about 26 m high, is characterized by a square plan with sides equal to about 4 m. The walls thickness is constant along the height and is equal to 0.8 m for the southern side and 0.65 for the other three sides; the bell tower presents a 1.3 m high basement characterized by a thickness that is 15 cm larger than the upper part. A small dome, which exhibits a diameter of about 3.65 m, is present on the top of the tower: it is supported by a circular tambour.
Two doors, which are 2.1 m high, and a small window, which is 0.5 m wide and 0.7 m high, are present at the ground level, respectively on the west, north and east sides: the south side does not exhibit any openings. Each side of the belfry presents a large arched opening that is 3.3 m high.
The lower part of the bell tower, up to a height of 17 m, is characterized by the presence of many decorative niches. In the upper part, two pilasters on each side enclose the bell openings.
Fig. 4 shows the elevation views of the four sides of Tower 3 along with the sections at relevant different heights with indications of the main geometrical dimensions.

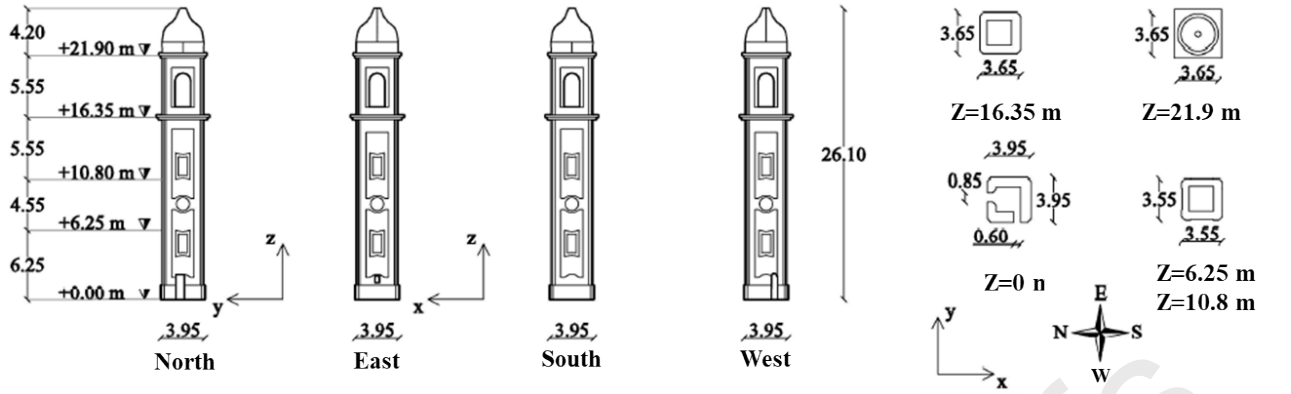

Fig. 4. Tower 3. Elevation views, plan and relevant sections of the bell tower with indication of the main geometrical dimensions.

2.4. Tower 4

The bell tower, which is about 29.4 m high, is characterized by a square plan with sides equal to 4.6 m. The walls thickness remains quite constant along the lower part of the bell tower with a minimum value equal to about 0.3 m for all the sides: a significant increase of the thickness can be observed on the four corners of the square section. A small dome, which exhibits a diameter of about 4.4 m, is present on the top of the tower: it is supported by an octagonal tambour that is almost 3 m high. In the lower part of the bell tower, up to a height of 20 m, only two small rectangular windows and the entrance door at the base are present on the south side. In the upper part of the bell tower, each side presents a large arched opening that is about 2.4 m high: in addition, each side of the tambour exhibits a rectangular opening that is about 2 m high. The bell tower is also characterized by the presence of decorative cornices at regular intervals and many rectangular recesses of 5-10 cm on each side, used as decorations and supports for statues.

Fig. 5 shows the elevation views of the four sides of Tower 4 along with the sections at relevant different heights with indications of the main geometrical dimensions.

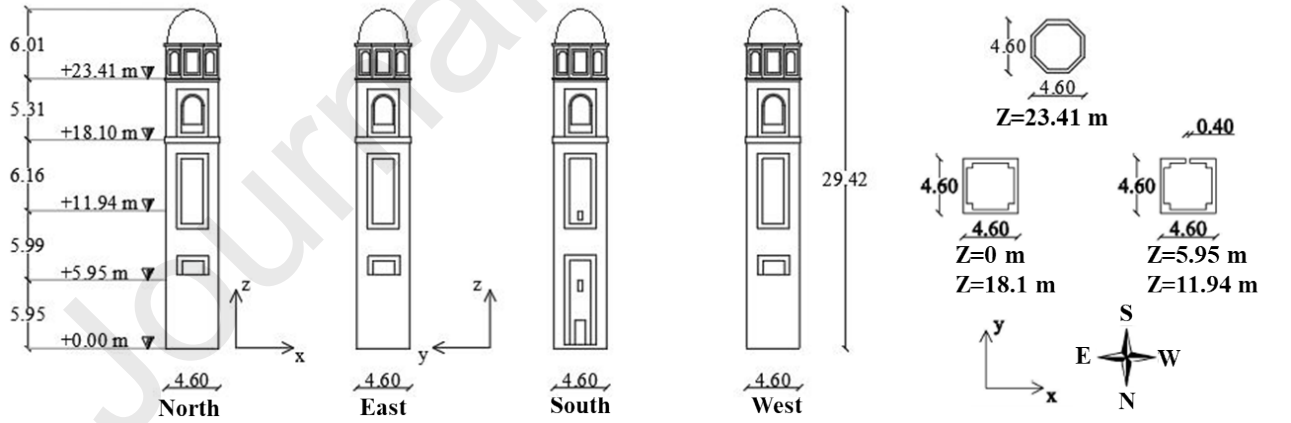

Fig. 5. Tower 4. Elevation views, plan and relevant sections of the bell tower with indication of the main geometrical dimensions.

2.5. Tower 5

The bell tower, which is 35.4 m high, is characterized by a square plan with sides equal to about 4.9 m. The walls thickness varies gradually along the height, from a maximum value of 0.95 m at the base to a minimum value of 0.4 m below the tambour. A small dome with a diameter of about 3.6 m is present on the top of the tower: it is supported by an octagonal tambour that is almost 4 m high.

On the north side, a 2.1 m high door is present at the base. On the east and south sides there are no openings in the lower part, but only a rectangular niche on the south side. On the west side there are a 2.5 m high door, a 1.2 m high rectangular window and a 2.1 m high arched window.
Above the height of 13 m, the bell tower is almost symmetric: a circular niche, which is 2.2 m high, and two wide arched windows, which are 2.9 m high, can be found on each side. Above them, each of the eight sides of the tambour presents an arched opening that is 2.4 m high.
The majority of the bell tower is characterized by the presence of decorative cornices at regular intervals and some 5-10 cm deep niches, especially around the openings; in addition, in the upper part two 4.5 m high pilasters are located near the arched openings.
Fig. 6 shows the elevation views of the four sides of Tower 5 along with the sections at relevant different heights with indications of the main geometrical dimensions.

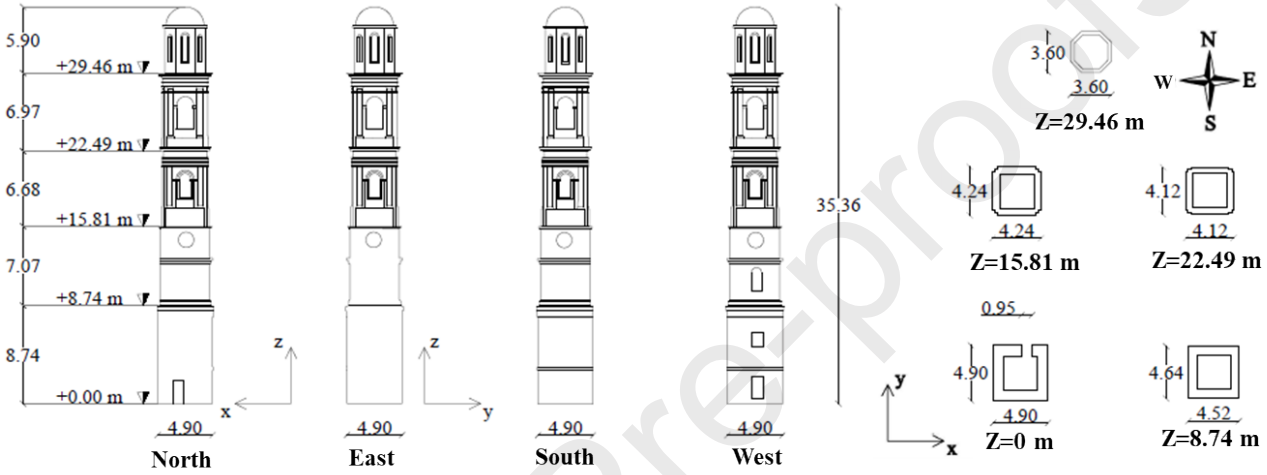

Fig. 6. Tower 5. Elevation views, plan and relevant sections of the bell tower with indication of the main geometrical dimensions.

2.6. Material characteristics

The masonry of the five bell towers is made with solid bricks and lime mortar. As already mentioned, in this study the same properties of masonry material were assumed for all the bell towers in order to have an insight into the seismic behavior of the structures particularly as a function of their geometry. The mechanical properties of masonry have been defined considering the provisions of the Italian Code [37-39] and are summarized in Table 1. The values of the modulus of elasticity (E) and shear modulus (G) are the average between the upper and lower bounds of the range suggested in [37-39], while the values of the compressive strength (f_m) and shear strength (τ_0) are the minimum.

Table 1. Mechanical properties assumed for masonry consisting of solid bricks and lime mortar.

f_m [N/mm^2]	τ_0 [N/mm^2]	E [N/mm^2]	G [N/mm^2]	w [kN/m^3]
2.4	0.06	1500	500	18

Notation: f_m = compressive strength, τ_0 = shear strength, E = modulus of elasticity, G = shear modulus, w = specific weight.

3. Preliminary seismic assessment through a simplified approach

For a preliminary evaluation of the seismic vulnerability of the bell towers under study, a simplified procedure based on the equivalent lateral static analysis suggested by the Italian Guidelines [39] is performed. A simplified mechanical model is assumed for the bell tower that is modelled as a cantilever beam subjected to a system of static horizontal forces. The model of the bell tower is divided into different blocks presenting uniform characteristics. The safety checks are carried out by

comparing, at the base of each block, the acting and resisting bending moments along the height of the structure. In order to evaluate the resisting bending moment, zero tensile stresses and a limited compressive strength are assumed for masonry.

The acting bending moment is computed through an equivalent static analysis, adopting a linear distribution of horizontal static forces along the height of the bell tower. The force to be applied in correspondence with the center of mass of each block is given by the following expression:

$$F_i = \frac{W_i z_i}{\sum_{k=1}^{n} W_k z_k} F_h \qquad \text{where} \qquad F_h = 0.85 \frac{S_e(T_1) W}{q \quad g} \tag{1}$$

where W_i and W_k denote, respectively, the weight of the i-th and k-th blocks, z_i and z_k are, respectively, the height of the centers of mass of the i-th and k-th blocks with respect to the tower foundations, $S_e(T_1)$ is the ordinate of the elastic response spectrum, which is function of the main period T_1 of the tower along the considered loading direction, q is the behavior factor, W is the total weight of the tower and g is the gravity acceleration. The resultant of the seismic forces acting at the i-th section is given by:

$$F_{hi} = \frac{\sum_{k=i}^{n} W_k z_k}{\sum_{k=1}^{n} W_k z_k} F_h \tag{2}$$

The acting bending moment is obtained from the following expression:

$$M_i = F_{hi}\left(\frac{\sum_{k=i}^{n} W_k z_k^2}{\sum_{k=1}^{n} W_k z_k} - z_i^*\right) \tag{3}$$

where z_k is the height of the center of mass of the k-th block (presenting weight W_k) and z_i^* is the height of the i-th section, which should be verified, with respect to the tower foundations.

In this study, the response spectra provided by Eurocode 8 [40] with three different soil types (soil types A, B, C) are considered. The behavior factor is assumed equal to 2.8, as suggested by the Italian Guidelines [39] for such typologies of structures in the case of stiffness irregularities along the height of the bell tower. According to the procedure, for bell towers with hollow section with approximately rectangular shape, simplified formulas can be adopted for the evaluation of the resisting bending moment. Under the assumption that the normal pre-compression does not exceed the value of $0.85 f_d A_s$, the ultimate bending moment at any cross-section can be evaluated as:

$$M_u = \frac{\sigma_0 A}{2}\left(b - \frac{\sigma_0 A}{0.85 a f_d}\right) \tag{4}$$

where b and a are the section sides in the longitudinal and orthogonal directions of the seismic action, A is the section area, σ_0 = W/A is the vertical compressive stress in the section (W is the tower weight above the section considered) and f_d is the design compressive strength of masonry, which is obtained according to the Italian Code [37-39]. The lowest knowledge level (LC1) is adopted for masonry.

The number of transversal sections considered to estimate the ultimate flexural strength is set equal to 20 for all the bell towers under study. The positions of transversal sections, where the cross-section strength is evaluated, are chosen in order to investigate the flexural behavior at meaningful locations, taking into account mainly the presence of openings and the thickness variation of masonry walls.

Fig. 7 shows the results of the comparison between resisting and acting bending moments in the two orthogonal directions at the critical sections of the five bell towers for different ground types (A, B, C) and various seismic intensity levels (Sa_g=0.05g, Sa_g=0.15g, Sa_g=0.25g, Sa_g=0.35g). The critical section is located at the base for Tower 1, Tower 2 and Tower 4: on the contrary, it is located at a

height of 1.45 m for Tower 3 due to the sharp restriction of the section and at a height of 0.5 m for Tower 5 due to the presence of large openings.

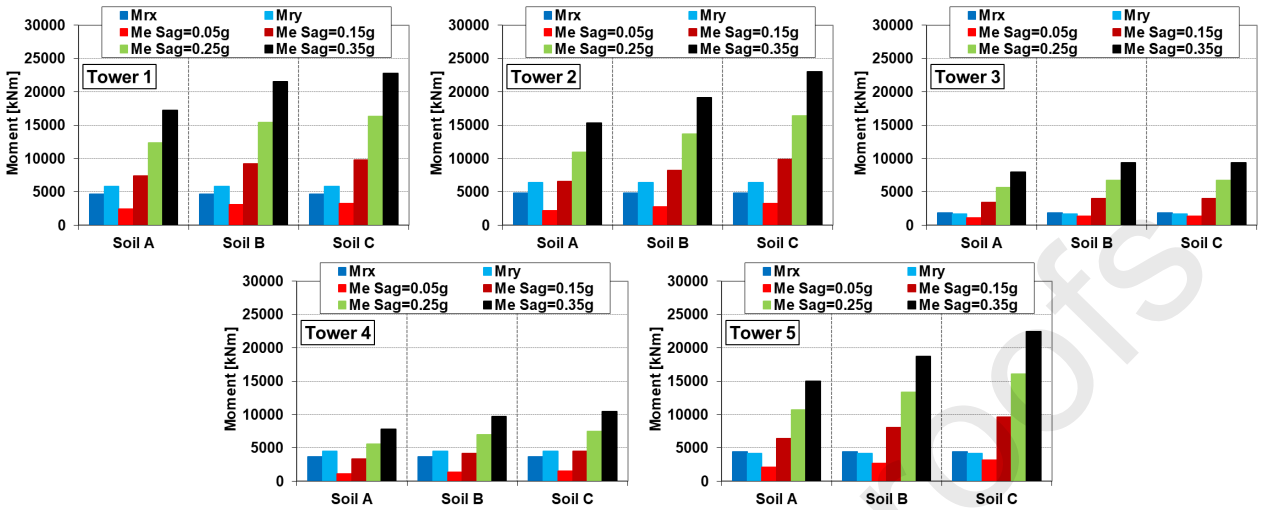

Fig. 7. Values of resisting (Mr) and acting (Me) bending moment obtained for the critical section of the different bell towers, considering different soil types and different seismic intensity levels.

According to the simplified procedure, the seismic safety Index is evaluated for the bell towers under consideration. The seismic safety Index can be defined as follows:

$$I_s = \frac{a_{SLU}}{a_g} \tag{5}$$

where a_{SLU} is the peak ground acceleration corresponding to the collapse of the structure and a_g is the design ground acceleration on ground type A. A value of the seismic safety Index greater than one corresponds to a safe state for the bell tower under consideration. This index is useful to provide a quantitative indication of any deficiency in terms of mechanical strength of the bell tower.
The values of the seismic safety Index obtained for the five bell towers under study are reported in Fig. 8 for both the directions and for four different seismic intensity levels (Sa_g).
-It can be noted that: (i) under Sa_g=0.05g, the seismic safety Index is larger than one for all the bell towers, considering all the ground types; (ii) under Sa_g=0.15g, the seismic safety Index is smaller than one for all the bell towers, except for Tower 4 in the case of ground type A; (iii) under Sa_g=0.25g and Sa_g=0.35g, the seismic safety Index is smaller than one for all the bell towers, considering all the ground types.
-The lowest values of the seismic safety Index are computed for Tower 3. The high seismic vulnerability of the bell tower is given mainly by the reduced ultimate moment resistance at the base, also due to the presence of large doors. As already mentioned, the critical section is located in correspondence with the sharp reduction of the base section (at a height of 1.4 m).
-Low values of the seismic safety Index are computed also for Tower 5. The high seismic vulnerability of the bell tower is due to the large mass of the structure generating high horizontal forces and consequently large values of acting bending moment at the base: moreover, the ultimate moment resistance at the base is reduced by the presence of openings (the door on the north side and the opening on the west side) in both the directions.
-The largest values of the seismic safety Index are computed for Tower 4. The low seismic vulnerability of the bell tower is mainly due to the low weight (the lowest weight among the different bell towers) of the structure that is related to small values of acting bending moment at the base.

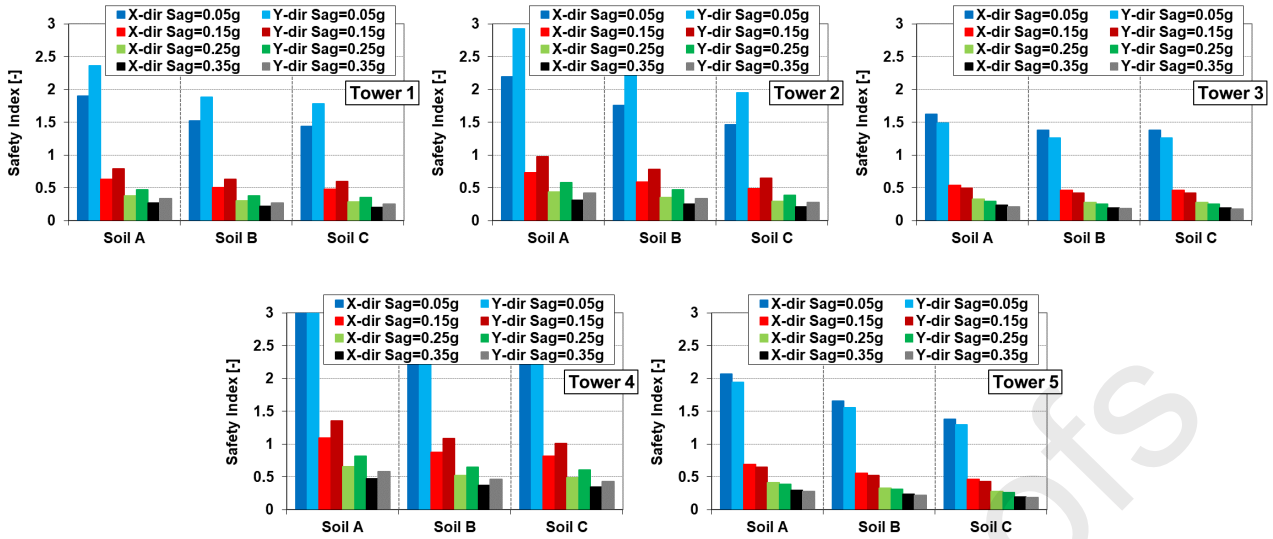

Fig. 8. Values of the seismic safety Index obtained through the simplified procedure at the base section of the different bell towers for different seismic intensity levels in the X and Y directions.

The seismic safety Index is also computed referring only to the belfry and the results are reported in Fig. 9 for each bell tower considering three different ground types.

-It can be noted that the seismic safety Index is larger than one for all the bell towers under Sa_g=0.05g and Sa_g=0.15g, considering all the ground types.

-The belfry of Tower 3 presents the lowest seismic safety Index, which is smaller than one for Sa_g=0.25g and Sa_g=0.35g for all the ground types. The high seismic vulnerability of the belfry is due to the reduced cross-section area, the notable mass on the top and, above all, the largest openings percentage among the different bell towers.

-The belfry of Tower 5 presents low values of the seismic safety Index, which is smaller than one for Sa_g=0.35g (for all the ground types) and for Sa_g=0.25g (for ground type C). The high seismic vulnerability is mainly due to the cross section and walls thickness reductions in the belfry.

-The lowest seismic vulnerability is observed for Tower 4, which does not present values of the seismic safety Index smaller than one for all the PGA values and for all the ground types. Such a result is mainly due to the small value of the openings percentage and the reduced mass in the upper part of the bell tower.

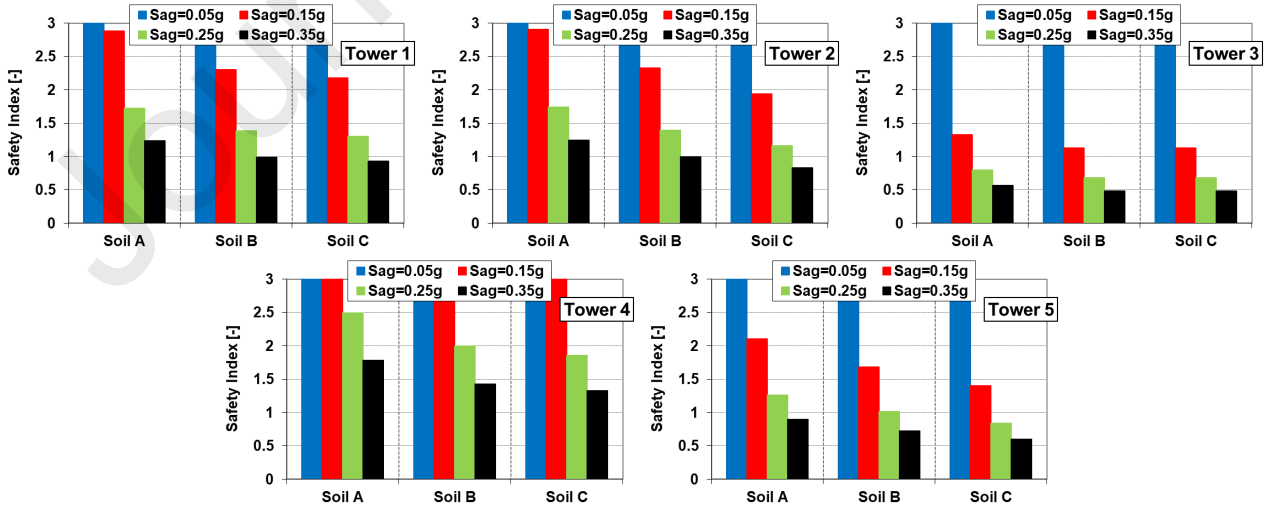

Fig. 9. Values of the seismic safety Index obtained through the simplified procedure at the belfry of the different bell towers for different seismic intensity levels.

4. FE models of the bell towers

Detailed three-dimensional FE models of the five bell towers under study were created through the software code Abaqus [41] using the drawings and the data collected from existing available documentations and during the survey phase. Fig. 10 shows the geometrical and FE models of the five bell towers. It is worth mentioning that the wooden structures of floors and stairs were not considered in the FE models. Four-node tetrahedral elements having a size ranging between 20 cm and 30 cm were used in the discretization of the models. Each FE model was subdivided in elevation into five different parts that have been investigated in detail in the following sections, Fig. 10. Table 2 summarizes the main characteristics of the FE models of the bell towers. It can be noted that the bell towers under study present a similar high slenderness that ranges between about 6.4 and 7.2.

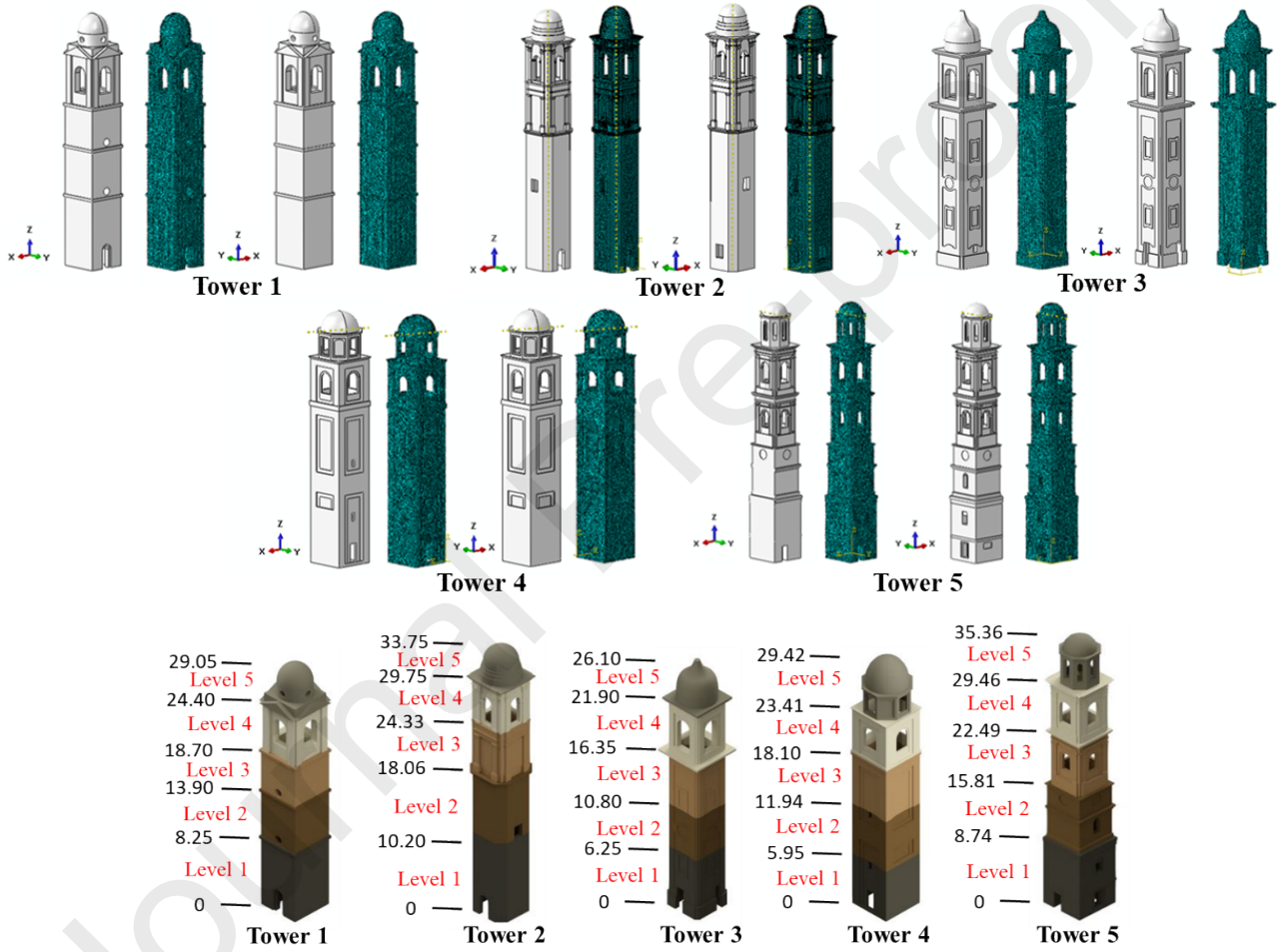

Fig. 10. Top: geometrical and FE models of the bell towers under study. Bottom: indication of the subdivision of the bell towers into five parts (Levels) in elevation.

Table 2. Main characteristics of the FE models of the bell towers.

	Number of elements [-]	Average element size [m]	Weight [kN]	Max dimension in plan [m]	Height [m]	Base walls thickness [m]	Minimum slenderness [-]	Base Area [m^2]	Openings percentage [%]
Tower 1	109256	0.3	6100	4.5 x 4.52	29.05	0.98-1.02	6.46	14.04	5.14
Tower 2	100353	0.3	4704	4.8 x 4.8	33.75	0.5	7.03	9.53	4.96
Tower 3	138960	0.25	3037	3.95 x 3.95	26.1	0.8-0.95	6.61	10.19	6.92
Tower 4	86695	0.25	2574	4.6 x 4.6	29.42	0.3-0.4	6.39	6.46	5.01
Tower 5	182035	0.25	5264	4.9 x 4.9	35.36	0.95	7.21	15.01	7.20

The non-linear behavior of masonry was defined adopting the Concrete Damaged Plasticity (CDP) model, which is available in ABAQUS/Standard [41]. A thorough description of the model and a comprehensive explanation of the values adopted for the main parameters can be found in previous works of the author [42-43]. The following relationships define the uniaxial tensile σ_t and compressive σ_c stresses:

$$\sigma_t = (1-d_t)E_0(\varepsilon_t - \varepsilon_t^{pl}) \qquad (6)$$
$$\sigma_c = (1-d_c)E_0(\varepsilon_c - \varepsilon_c^{pl})$$

where E_0 is the initial elastic modulus, ε_t and ε_c are the total strains in tension and in compression, ε_t^{pl} and ε_c^{pl} are the equivalent plastic strains in tension and in compression, d_t and d_c are the scalar damage variables in tension and in compression. Fig. 11 shows the stress-strain relationships of the CDP model adopted for masonry in tension and compression. As already explained, the main mechanical properties of masonry are assumed by referring to the indications provided in the Italian recommendations for existing buildings and built heritage [37-39]. In particular, according to Table 8.2.1 in the Explicative Notes to the Italian code [38], which provides reference values for the main mechanical properties of different typologies of masonry, the following assumptions are made for a masonry consisting of solid bricks and lime mortar: (i) the compressive strength is equal to σ_{cu}=2.4 MPa; (ii) the elastic modulus is equal to 1500 MPa; (iii) the specific weight is equal to 18 kN/m^3. The tensile strength is assumed equal to σ_{to}=0.24 MPa, considering a ratio between the tensile and compressive strength equal to 0.1. The scalar damage variable in tension (d_t), representative of the stiffness degradation of the material, is assumed to vary linearly: the values range from zero, for the strain corresponding to the stress peak, to 0.95, for the ultimate strain value of the softening branch. Table 3 specifies the uniaxial stress-strain values assumed in compression and in tension for masonry and the evolution of the scalar damage variable in tension.

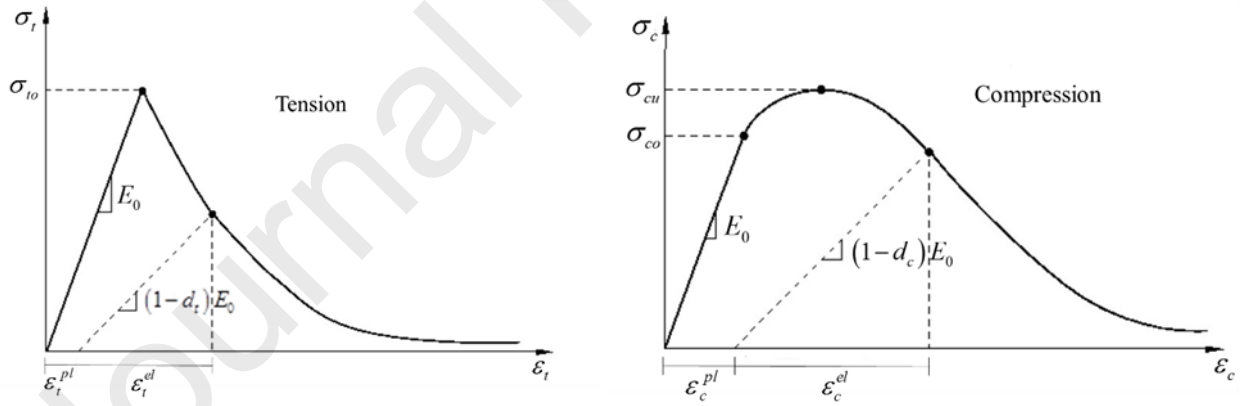

Fig. 11. Representation of the masonry constitutive behavior in tension and compression.

Table 3. Uniaxial stress–strain values and scalar damage values utilized in the CDP model for masonry.

Compression		Tension		Damage in tension	
Stress [MPa]	Inelastic strain [-]	Stress [MPa]	Cracking strain [-]	d_t	Cracking strain [-]
1.9	0	0.240	0	0	0
2.4	0.0053	0.120	0.00025	0.95	0.00121
0.96	0.0107	0.030	0.00057		
0.48	0.032	0.015	0.00121		

A preliminary evaluation of the dynamic behavior of the five bell towers can be obtained from modal analysis. Fig. 12 shows the deformed shapes and corresponding periods of the first five vibration modes of the five bell towers with an indication of the participating mass ratios. The results indicate that a similar dynamic behavior can be observed for all the bell towers: the first two modes, which are translational modes with relevant participating mass ratio along the two orthogonal directions, present similar periods, while the third mode presents a much smaller period. In particular, the period of the first mode is within the range 0.76 s - 0.88 s for the majority of the bell towers, except for Tower 2 that is characterized by a slightly larger period (1.04 s). Consequently, the bell towers present the first two modes with high participating mass ratio in correspondence with the beginning of the first descending branch of the response spectra (considering soil types A, B, C) and quite relevant spectral accelerations can be generally expected. Finally, it is worth mentioning that the values of the fundamental period obtained from modal analysis for the FE models of the bell towers under study are generally higher than the values obtained using empirical formulas proposed by codes or developed using ambient vibration tests in the literature and reported in [44-47]. It can be noted that the difference of values is larger especially for the simplified empirical formulas in which the main natural frequency is expressed as a function of only the total height of the tower. On the other hand, the fundamental period obtained from modal analysis is in a good agreement, for the majority of the bell towers under study, with the following empirical formula suggested in [46], which expresses the fundamental period as a function of the maximum slenderness evaluated as the ratio between the total height of the tower (H) and the minimum length of the outer side of the base cross section (B):

$$T_1 = \frac{1}{Y\left(\frac{H}{B}\right)^{-z}} \tag{7}$$

Based on experimental data, the values of Y and z are assumed equal to 3.58 and 0.57, respectively, for masonry tower structures [46]. The empirical formula provides values of the fundamental period of the bell towers under study within the range 0.80 s - 0.86 s, as shown in Table 4: for each bell tower, except Tower 2, the difference between the value obtained from FE models and the one estimated through the empirical formula is smaller than 5%. It is worth mentioning that Tower 2 presents an approximately octagonal plan (with respect to the square plan of all the other towers) with small base walls thickness.

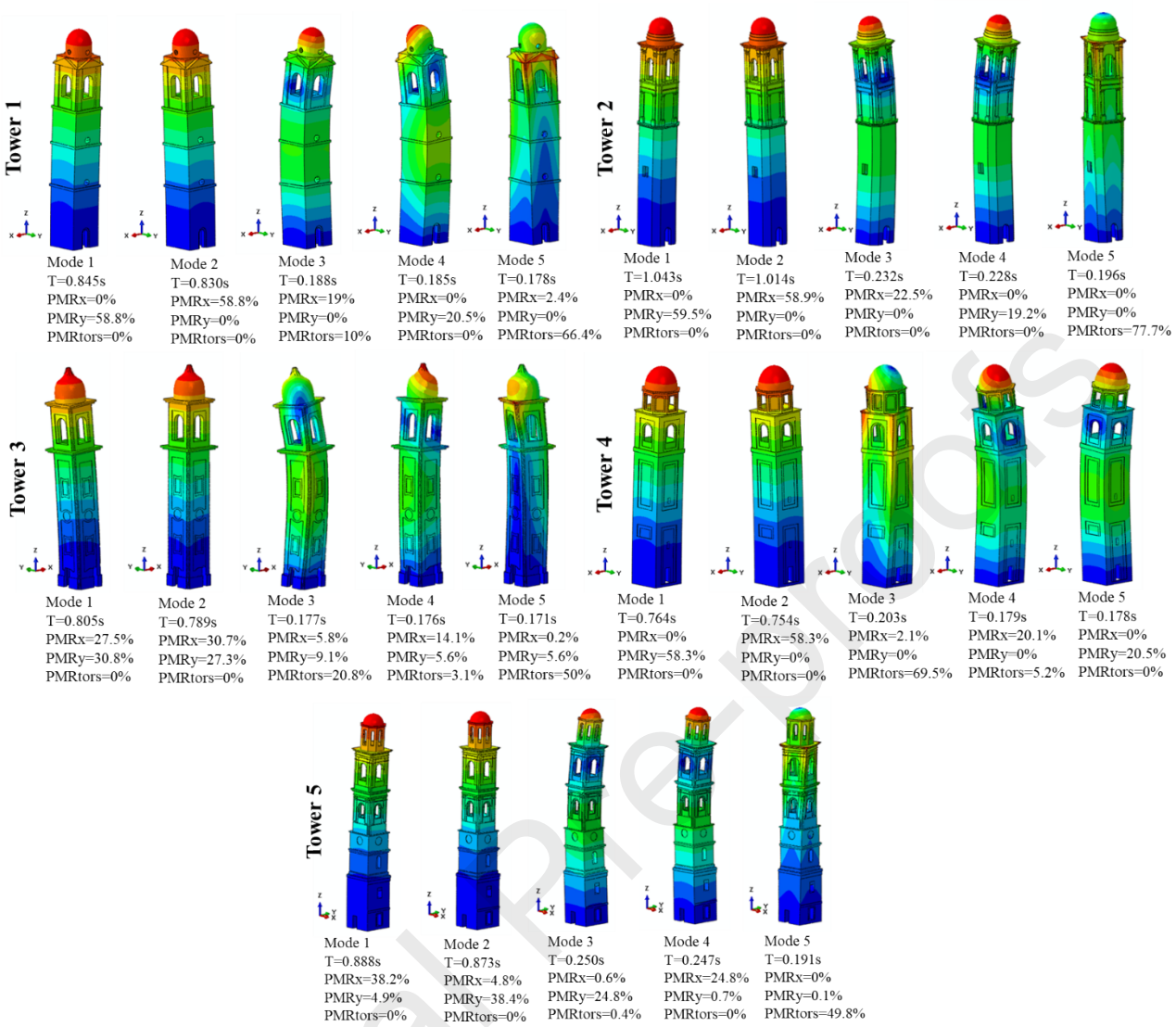

Fig. 12. Deformed shapes and corresponding periods of the first five vibration modes of the different bell towers with indication of the participating mass ratios (PMR).

Table 4. Fundamental period [s] of the bell towers under study obtained from FE models and estimated through the empirical formula proposed in [46].

	Tower 1	Tower 2	Tower 3	Tower 4	Tower 5
FE model	0.845	1.043	0.805	0.764	0.888
Shakya (2014)	0.809	0.849	0.820	0.804	0.861

5. Non-linear dynamic analyses

The seismic response of the masonry bell towers under study was assessed through bi-directional non-linear dynamic analyses with response spectrum-compatible artificial accelerograms and real accelerograms. The set of artificial ground motions consisted of three different pairs of records that were generated so as to match different Eurocode 8 response spectra (Type 1, 5% viscous damping) using the computer code SIMQKE [48]: three ground types (A, B, C in accordance with Eurocode 8) and four PGA values (PGA=0.05g, PGA=0.15g, PGA=0.25g, PGA=0.35g) were considered. In addition, the real accelerograms registered on May 29 during the 2012 Emilia seismic sequence (Mirandola station) were also used. The same accelerograms, which present equal intensity in the two

orthogonal directions, were adopted for the numerical simulations of the seismic response of all the bell towers. The time-history accelerations (denoted as AccA, AccB, AccC as a function of the ground type, and AccM for Mirandola station) and the corresponding response spectra (for PGA=0.15g) used in this study are shown in Fig. 13. It is worth mentioning that the vertical component of the seismic action is not considered in the nonlinear dynamic analyses to better compare the results with the simplified method that does not take into account such a component.

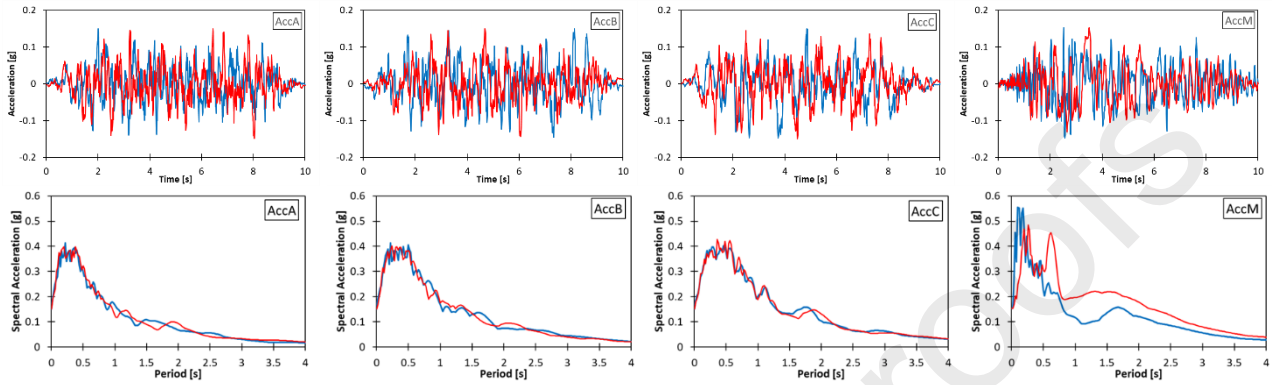

Fig. 13. Horizontal components (component blue applied in the X direction and component red applied in the Y direction) of the accelerograms used in the non-linear dynamic analyses and corresponding acceleration response spectra.

5.1. Displacements

Fig. 14 shows the maximum normalized displacements (top displacement/height) registered in the X and Y directions for the five bell towers during the non-linear dynamic analyses under the different accelerograms with various PGA values.

-The largest normalized displacements are registered for Tower 3 under all the accelerograms. It can be noted that Tower 3 presents the smallest base section sides and the largest openings percentage at the base (Level 1) and in the belfry (Level 4). Large normalized displacements are also generally observed for Tower 4, which is characterized by the smallest base area and reduced walls thickness along the whole height. It is worth mentioning that both Tower 3 and Tower 4 exhibit the smallest values of the fundamental period corresponding to the highest values of spectral accelerations.

-The largest normalized displacements are registered for Tower 1, Tower 2 and Tower 3 under AccM and for Tower 4 and Tower 5 under AccC. On the other hand, the smallest normalized displacements for all the bell towers are computed under AccA. It is important to point out that, considering the values of the fundamental periods of the bell towers under study, the lowest spectral acceleration amplifications are registered under AccA.

-It can be noted that under AccM the largest normalized displacements are observed in the Y direction for all the bell towers, meaning that the component of AccM applied along the Y direction is more severe than the component applied along the X direction. In particular, a large difference of normalized displacements in the two directions is observed for Tower 3 under both PGA=0.25g and PGA=0.35g.

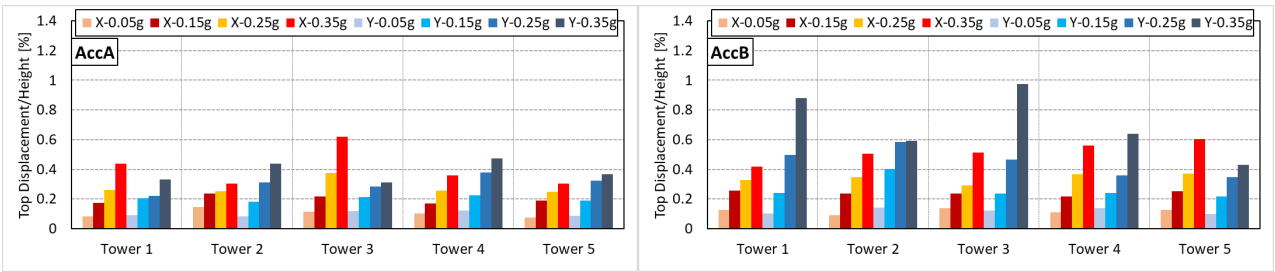

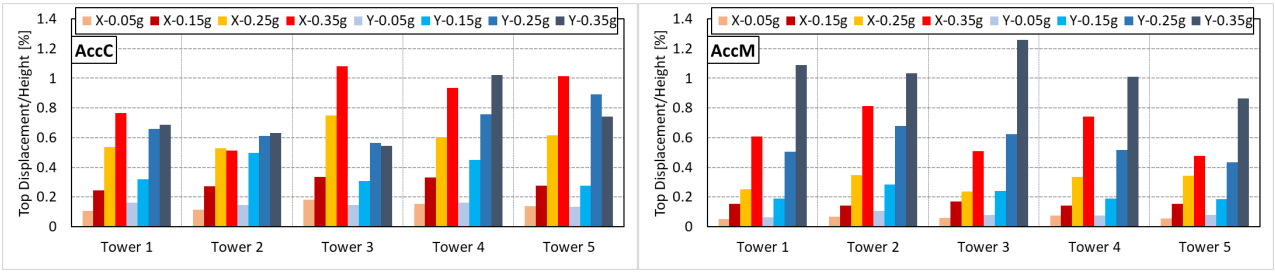

Fig. 14. Maximum normalized displacements (top displacement/height) registered in the X and Y directions for the five bell towers during the non-linear dynamic analyses under the different accelerograms with various PGA values.

5.2. Damage contour plots

Figs. 15-19 show the tensile damage contour plots of the five bell towers at the end of the non-linear dynamic analyses under the different accelerograms considering various PGA values. The following sub-sections describe the evolution of tensile damage for each bell tower: the last sub-section provides an overall analysis of the main results in terms of tensile damage contour plots for the five bell towers.

5.2.1. Tower 1

-Under PGA=0.05g, some small cracks, which originate from the large openings, are visible in the upper part of the bell tower, for all the accelerograms. Moreover, in the case of AccC and AccB, some small horizontal cracks can be observed at the base of the bell tower.
-Under PGA=0.15g, several sub-horizontal cracks can be detected at the base of the bell tower for all the accelerograms: it can be noted that they are more evident for AccB and AccC. The cracks observed at Level 4 propagate into the lower Level 3 for all the accelerograms.
-Under PGA=0.25g and PGA=0.35g, vertical and diagonal cracks spread along the height, involving also the middle part of the bell tower. It is interesting to observe that, passing from PGA=0.25g to PGA=0.35g, the highest increase of damage is registered under AccM. The dome presents negligible damage for all the accelerograms.

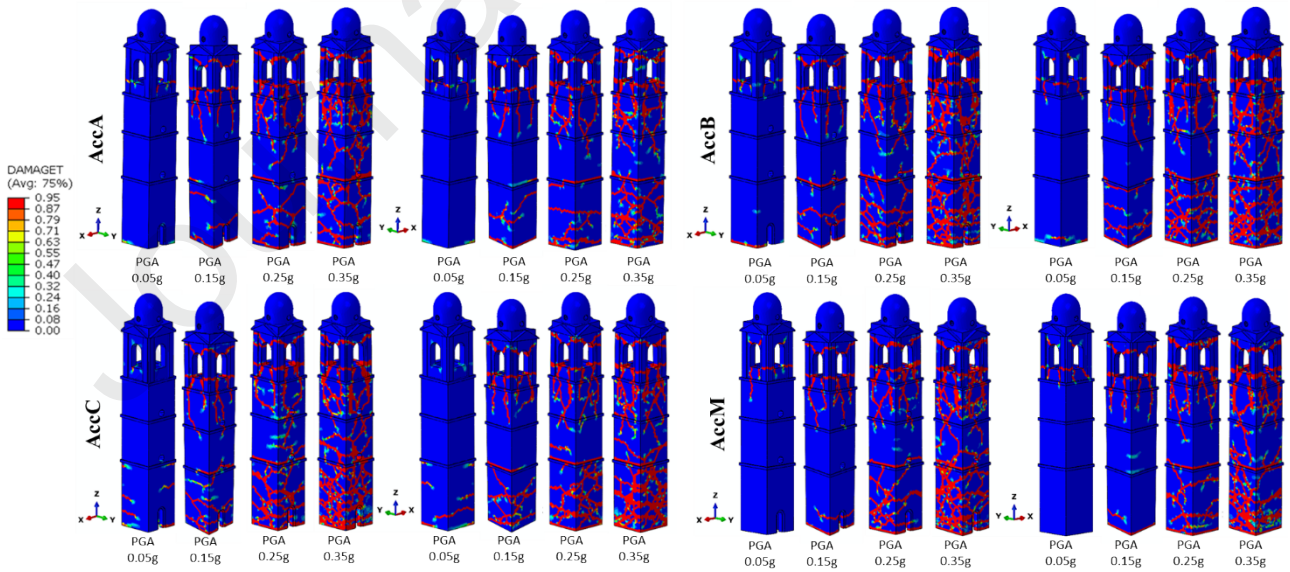

Fig. 15. Tower 1. Tensile damage contour plots at the end of the non-linear dynamic analyses for different accelerograms with various PGA values.

5.2.2. Tower 2

-Under PGA=0.05g, some small vertical cracks can be observed in correspondence with the small openings located at Level 2 for all the accelerograms, also due to the reduced walls thickness. Some first small cracks, which originate from the large openings, are observed in the belfry for the case of AccM and AccC. An onset of horizontal cracks can be detected at the base of the bell tower for all the accelerograms.
-Under PGA=0.15g, several cracks can be observed near the large openings of the belfry for all the accelerograms: they start to propagate towards the lower part (Level 3). The cracks in correspondence with the small openings of Level 2 significantly extend into the neighboring parts for all the accelerograms and several cracks are registered at the tower base.
-Under PGA=0.25g and PGA=0.35g, extensive damage propagates in the middle and bottom parts of the bell tower, with a considerable damage concentration in the region (Level 1) below the small openings for all the accelerograms. Relevant cracks, which propagate into the dome in some cases, are observed in the upper part of the bell tower.

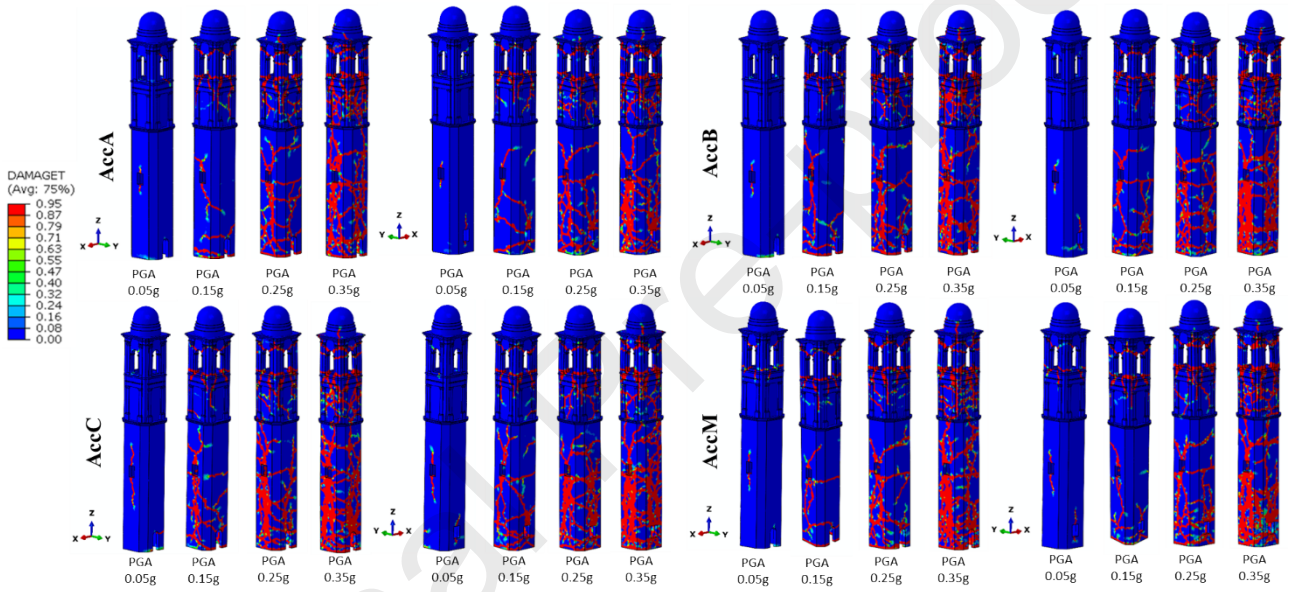

Fig. 16. Tower 2. Tensile damage contour plots at the end of the non-linear dynamic analyses for different accelerograms with various PGA values.

5.2.3. Tower 3

-Under PGA=0.05g, some first small cracks are registered near the large openings of the belfry, especially for AccM and AccC. A clear horizontal crack is also detected in correspondence with the sharp reduction of the section near the base, except for the case of AccM.
-Under PGA=0.15g, a significant increase of damage is observed in the belfry for all the accelerograms and several horizontal and diagonal cracks appear at the base, especially in the case of AccC. The horizontal crack registered in correspondence with the reduction of the section near the base is more evident.
-Under PGA=0.25g and PGA=0.35g, a further increase of damage is observed especially in the upper part and at the base of the bell tower, with some cracks that are clearly visible also in the middle part. The dome at the top presents negligible damage for all the accelerograms.

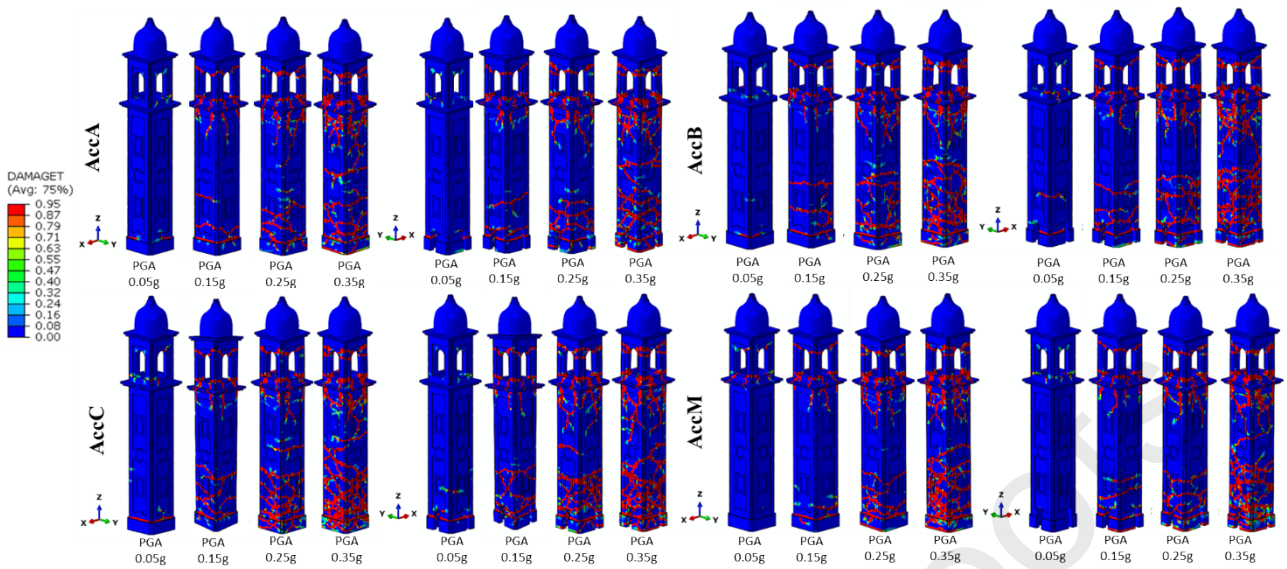

Fig. 17. Tower 3. Tensile damage contour plots at the end of the non-linear dynamic analyses for different accelerograms with various PGA values.

5.2.4. Tower 4

-Under PGA=0.05g, several vertical cracks are observed in the belfry (Level 4) for all the accelerograms: differently from the other bell towers, such cracks propagate in the lower part along the height of the bell tower due to the reduced walls thickness, even for small PGA values. Small horizontal cracks are also detected at the tower base for all the accelerograms, except for AccM.
-Under PGA=0.15g, an increase of the vertical and diagonal cracks in the belfry and in the lower parts is observed for all the accelerograms. Moreover, several cracks originate from the door at the base of the bell tower and some small cracks are detected in the dome.
-Under PGA=0.25g and PGA=0.35g, a significant damage increase can be observed in the different parts, especially along the height of the structure. A uniform distribution of damage, which is more widespread than the one observed in the other bell towers, is registered for PGA=0.35g. It can be noted that damage is slightly less marked in the case of AccA. Moreover, several cracks can be observed in the dome for all the accelerograms.

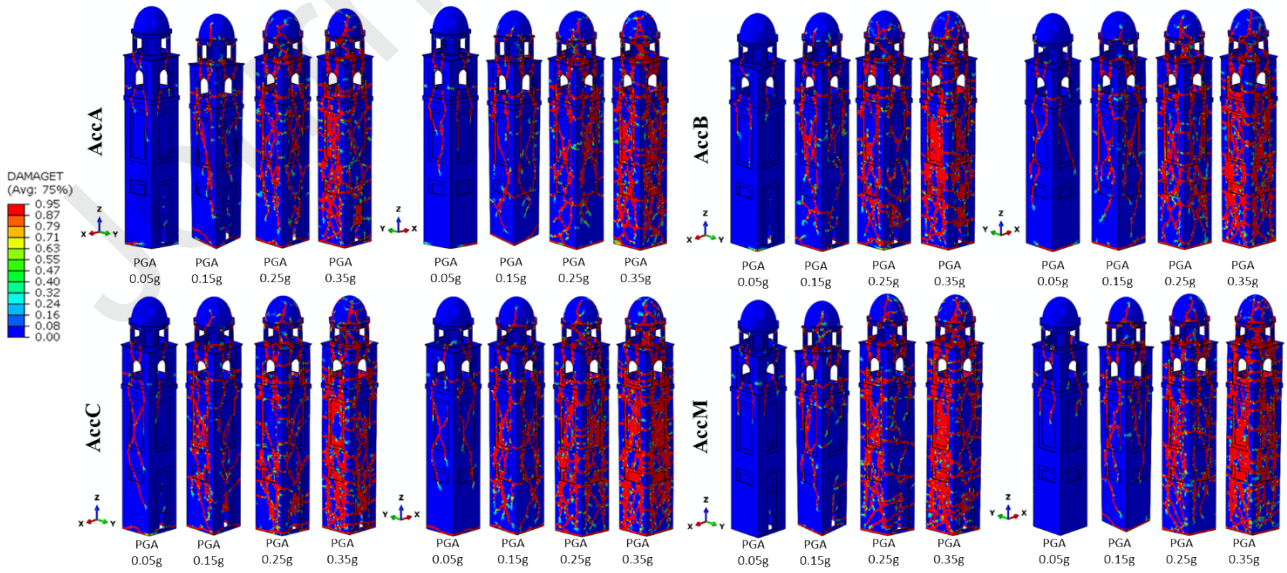

Fig. 18. Tower 4. Tensile damage contour plots at the end of the non-linear dynamic analyses for different accelerograms with various PGA values.

5.2.5. Tower 5

-Under PGA=0.05g, some cracks are observed in the upper part (Level 5) for all the accelerograms: damage involves also the regions (Levels 3 and 4) located underneath, in the case of AccB and AccC. An onset of small cracks is detected at the tower base only in the case of AccC.
-Under PGA=0.15g, some horizontal cracks can be observed at the tower base for all the accelerograms. As in the case of Tower 3, a clear horizontal crack is registered in correspondence with the section reduction at the base of Level 2. Damage significantly extends at Level 5 and involves the openings of the three upper parts for all the accelerograms.
-Under PGA=0.25g, damage concentrates mainly in the three upper parts with reduced walls thickness for all the accelerograms. Several cracks originate from the openings of the bottom part (Level 1 and Level 2) of the bell tower.
-Under PGA=0.35g, a widespread damage is observed in the three upper parts and a considerable increase of cracks is registered at Level 2 for all the accelerograms. Moreover, it is possible to observe a significant horizontal propagation of the cracks starting from the doors and openings at the base. In particular, a marked damage concentration is detected between the two openings at the base of the west wall in the case of AccM.

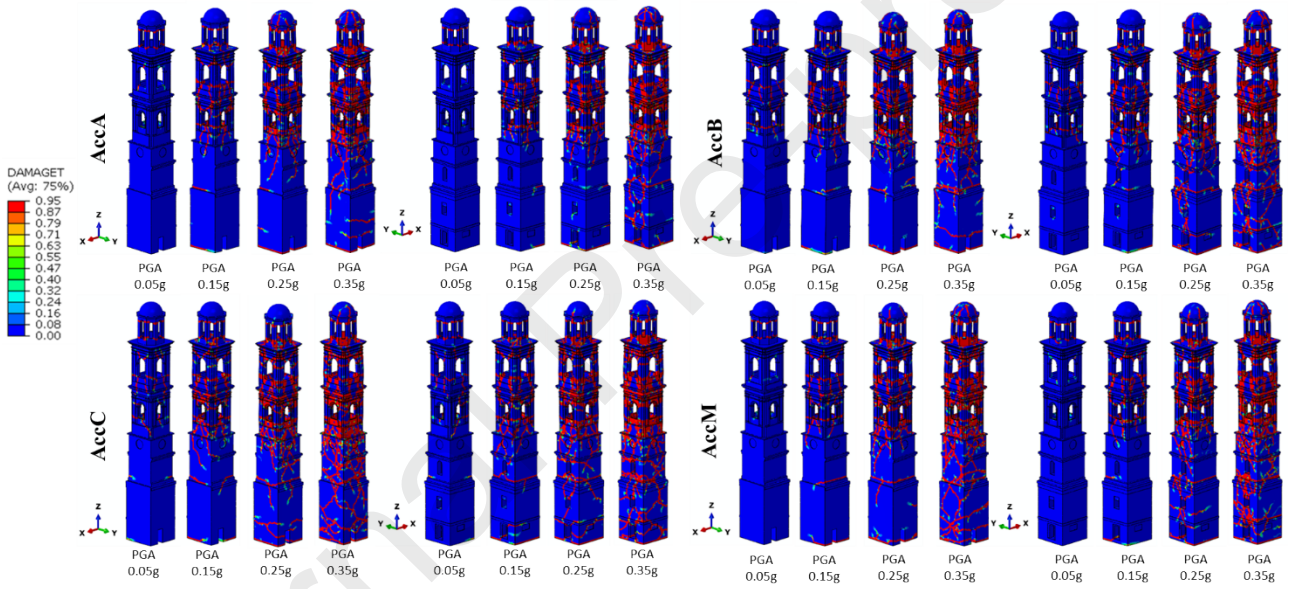

Fig. 19. Tower 5. Tensile damage contour plots at the end of the non-linear dynamic analyses for different accelerograms with various PGA values.

5.2.6. Overall analysis of results in terms of damage contour plots

From a careful analysis of the results in terms of tensile damage contour plots, it is worth mentioning that a similar onset and propagation of damage can be observed for the majority of the bell towers.
-Under PGA=0.05g, damage is restricted to only some small structural parts of the bell towers: in the majority of the bell towers, an onset of damage is observed in all four sides near the large openings of the belfry and some first horizontal cracks are detected at the tower base.
-Under PGA=0.15g, an increase of damage can be observed near the openings of the belfry and at the base of the bell tower. In some cases, the cracks of the upper parts begin to spread in the lower parts.
-Under PGA=0.25g, several vertical cracks are registered along the body of the bell towers and under PGA=0.35g a severe widespread damage distribution is clearly visible for all the bell towers.
-Tower 4 and Tower 5 show significant damage in the upper part (Level 5), mainly due to the reduced walls thickness and large openings percentage. On the other hand, Tower 5 presents limited damage at the base due to the large walls thickness, even for PGA=0.35g.

-Tower 2 and Tower 4 show a clear damage propagation from the belfry to the body of the bell tower due to the reduced walls thickness. A similar damage propagation along the height is observed also for Tower 5, due to also the presence of large openings.
-A very widespread damage concentration can be observed in the bottom part of Tower 2 and along the height of Tower 4 due to their small walls thickness, for PGA=0.35g.
-In the case of AccM, it is important to observe that, for all the bell towers, the two walls arranged along the Y direction present more damage than the two walls arranged along the X direction. This result is due to the different characteristics of the two components of AccM: the component applied in the Y direction causes more damage in the bell towers than the component applied in the X direction.

5.3. Energy density dissipated by tensile damage

Fig. 20 shows the energy density dissipated by tensile damage (EDDTD) for the five bell towers at the end of the non-linear dynamic analyses under the different accelerograms with various PGA values.
-For all the bell towers, the EDDTD values are significantly smaller under AccA than the other accelerograms, as already observed in terms of normalized displacements.
-The largest EDDTD value is registered for Tower 4 under all the accelerograms. As already noted from tensile damage contour plots, damage is distributed uniformly along the whole walls of the bell tower and is present also in the dome, which, on the contrary, exhibits negligible damage for the majority of the bell towers. Such results are consistent with the large displacements observed for Tower 4.
-Large EDDTD values are generally computed also for Tower 5, especially under AccA, AccB and AccC.
-The smallest EDDTD value is registered for Tower 3 under all the accelerograms and, most visibly, under AccC and AccM. This result is mainly due to the absence of openings in the central body of the bell tower and to the constant walls thickness (0.6 m) along the height. Such more regular configuration along the height of the bell tower does not provide preferential paths of damage propagation, preventing an extensive spread of the damage observed in the belfry and in the bottom part: moreover, the enlargement of the base section is effective in limiting the crack propagation at the base and around the entrance door. In addition, it can be noted that in Tower 3, differently from Tower 4 and Tower 5, damage is not present in the upper part (Level 5). It can be noted that the smallest EDDTD values are not consistent with the largest displacements observed for Tower 3.

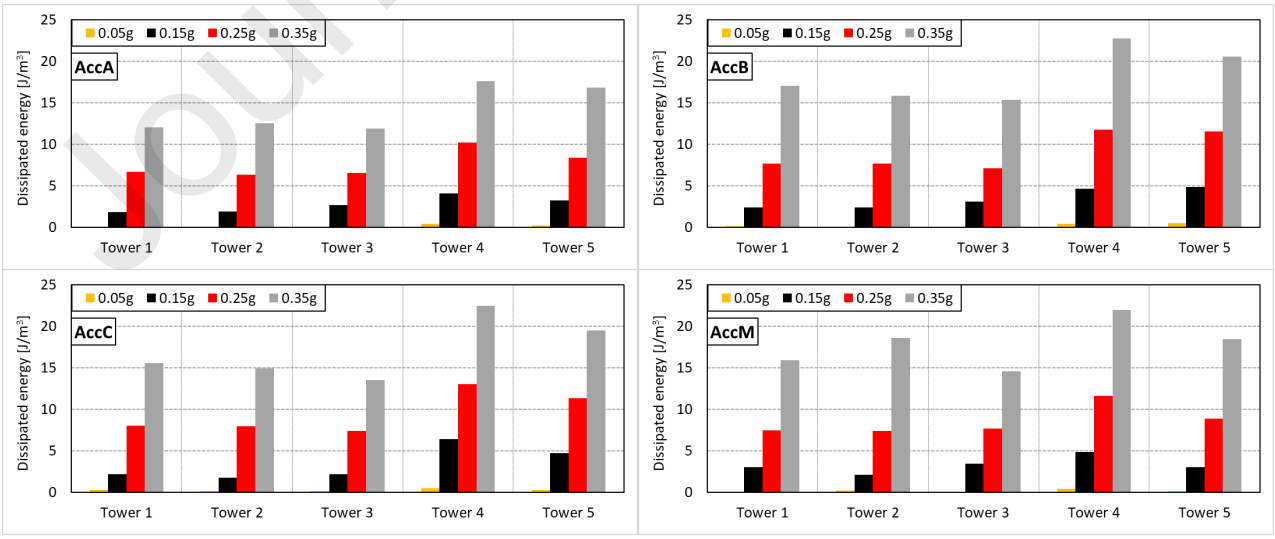

Fig. 20. Energy density dissipated by tensile damage (EDDTD) for the five bell towers at the end of the non-linear dynamic analyses under different accelerograms with various PGA values.

Fig. 21 shows the energy density dissipated by tensile damage (EDDTD) in the different five parts of the bell towers at the end of the non-linear dynamic analyses under the different accelerograms with PGA=0.15g and PGA=0.35g.

-It can be noted that a significant damage concentration is registered in the three upper parts (Levels 3-4-5) of Tower 5 for all the accelerograms. Such a result can be explained by the presence of large openings and the notable reduction of the walls thickness in the upper parts. It is interesting to point out that similar EDDTD values are observed for all the accelerograms, especially under PGA=0.35g.

-Among the different bell towers, the lowest EDDTD values in the bottom parts (Levels 1-2) are registered for Tower 5 for all the accelerograms. It can be noted that Tower 5 presents large walls thickness at the base, the longest base section sides and the largest base area.

-Tower 4 presents a more uniform damage distribution along Levels 2-5 among the different bell towers for all the accelerograms, especially under PGA=0.35g. In particular, a large increase of the EDDTD values is registered at Level 2 under PGA=0.35g with respect to lower PGA values. Moreover, the highest EDDTD values in the bottom parts (Levels 1-2) or in the lowest part (Level 1) are generally observed for Tower 4 for the majority of the accelerograms.

-It can be noted that high EDDTD values in the top part (Level 5) are registered only for Tower 5 and Tower 4, due to the presence of large openings. It is important to point out that, for all the other bell towers, Level 5 is composed of only the large dome without openings and damage is negligible.

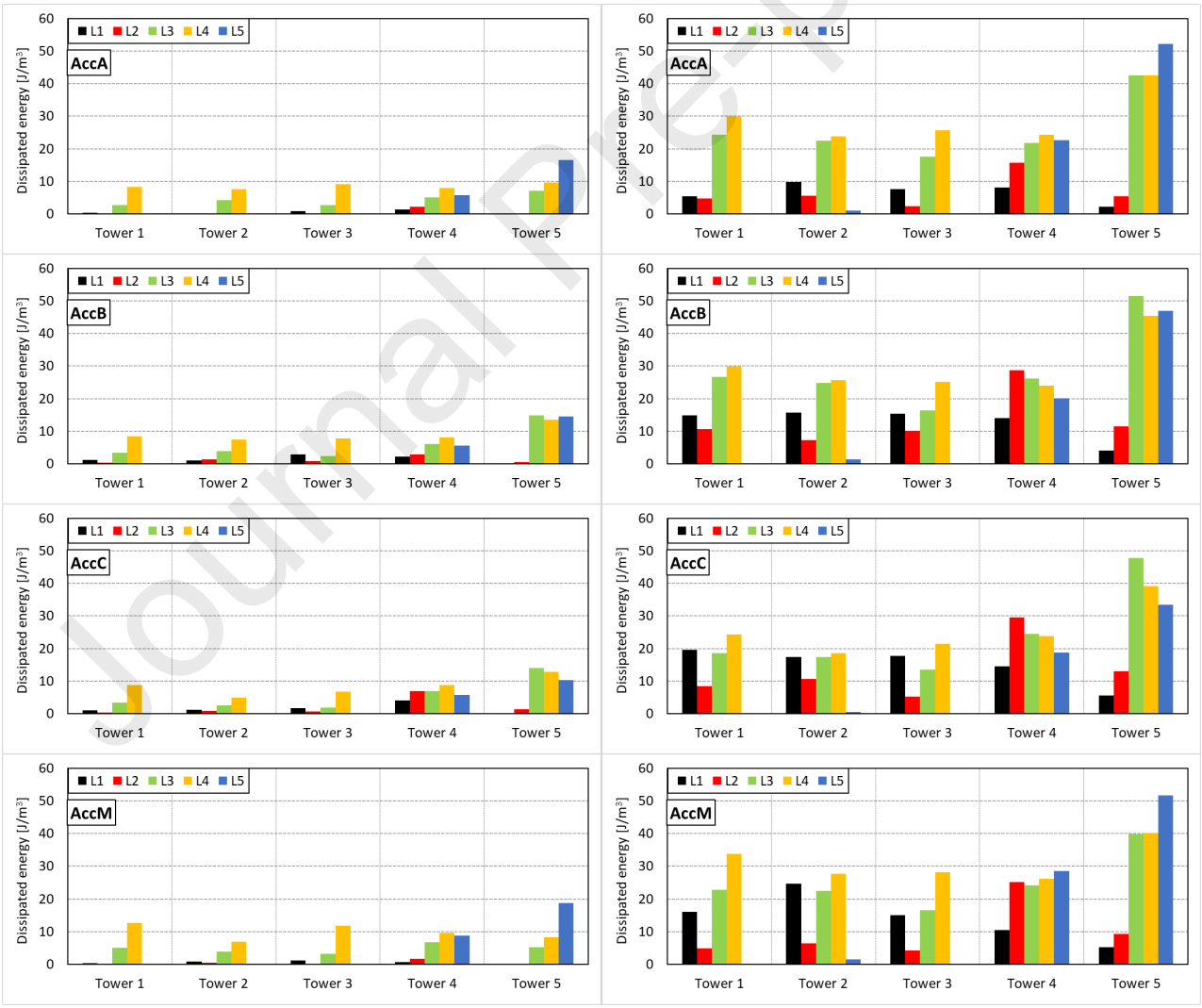

Fig. 21. Energy density dissipated by tensile damage (EDDTD) in the five parts of the bell towers at the end of the non-linear dynamic analyses under different accelerograms with two PGA values (PGA=0.15g and PGA=0.35g).

6. Comparison and discussion of results

6.1. Displacements

Fig. 22 shows the average values of the maximum normalized displacements (top displacement/height) registered in the X and Y directions for the four accelerograms and for the five bell towers during the non-linear dynamic analyses with different PGA values.

-It can be noted that the different characteristics of the accelerograms remarkably affect the maximum normalized displacements of the bell towers. As a matter of fact, a significant difference of maximum normalized displacements of the bell towers can be observed for the different accelerograms: the maximum normalized displacement registered under AccA is equal to about 0.4%, while the maximum normalized displacement registered under AccM is equal to about 1%.

-A considerable difference of maximum normalized displacements of the bell towers in the two (X and Y) directions is observed in case of AccM, especially under PGA=0.25g and PGA=0.35g. Such a result explains the largest values of the average normalized displacements computed in the Y direction for the majority of the bell towers.

-The difference of maximum normalized displacements is more limited considering the different bell towers with respect to the case of different accelerograms. In fact, it can be noted that the maximum values of normalized displacements under PGA=0.35g are within the range 0.6% and 0.8% for the five bell towers and within the range 0.4% and 1% for the different accelerograms.

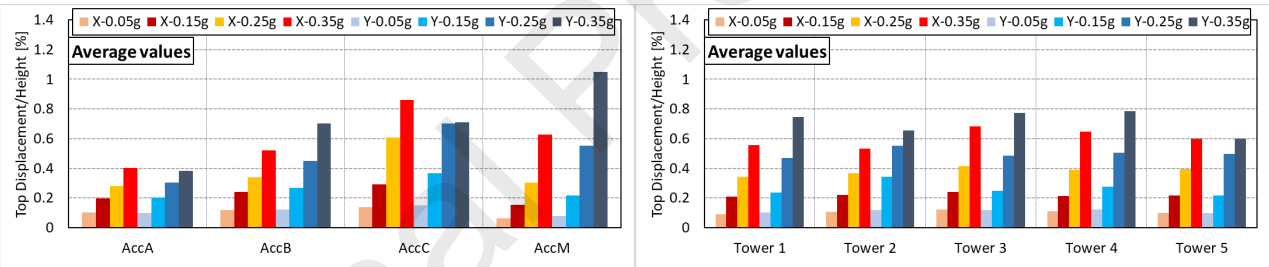

Fig. 22. Average values of the maximum normalized displacements (top displacement/height) registered in the X and Y directions for the four accelerograms (left) and for the five bell towers (right) during the non-linear dynamic analyses with different PGA values.

6.2. Onset and propagation of damage

As already mentioned, a similar onset of cracks and damage propagation can be identified for the majority of the bell towers. For small PGA values, it is possible to observe vertical and diagonal cracks starting from the large openings of the upper parts of the bell towers: then, for higher PGA values, cracks propagate along vertical or inclined paths into the lower parts of the bell towers. In addition, for small PGA values, horizontal cracks due to tensile stresses can be detected in the bottom parts in correspondence with the base. For high PGA values, widespread damage distributions are registered along the whole height of the bell towers, especially in presence of reduced walls thickness, as in the case of Tower 2 and Tower 4. Moreover, remarkable damage concentrations due to vertical irregularities can be detected in correspondence with sharp sections reductions along the height, as observed for Tower 1 and Tower 5 at the base of Level 2 and for Tower 3 in correspondence with the section reduction in proximity of the base.

6.3. Energy dissipated by tensile damage

Fig. 23 shows the average values of the energy density dissipated by tensile damage (EDDTD) for the four accelerograms and for the five bell towers at the end of the non-linear dynamic analyses with different PGA values.

-The EDDTD values are smaller in the case of AccA than in the cases of the other accelerograms, for all the PGA values: it can be noted that such a difference increases for higher PGA values. It is important to point out that the lowest spectral acceleration amplifications are registered in the case of AccA for all the bell towers, proving that the characteristics of the accelerograms may significantly affect the damage level in the bell tower.

-The largest EDDTD values are registered for Tower 4 and Tower 5. It is worth mentioning that Tower 4 is characterized by the smallest volume and presents the smallest walls thickness at the base: moreover, such a small wall thickness characterizes the whole height of the bell tower. On the other hand, Tower 5 exhibits large openings in the middle-upper parts (Levels 3-5) and a notable walls thickness reduction along the height. As a consequence, a significant difference should be highlighted: Tower 4 presents severe uniform distributions of damage along the height of the structure, while Tower 5 exhibits considerable damage concentrations in the middle-upper parts near the large openings.

-It is worth mentioning that a clear correlation between large normalized displacements and EDDTD values does not clearly emerge from the results obtained. In fact, Tower 3, which exhibits the largest normalized displacements, shows the lowest EDDTD values among the bell towers. On the contrary, Tower 4, which exhibits large normalized displacements, shows the highest EDDTD values among the bell towers because of severe uniform distributions of damage along the whole height.

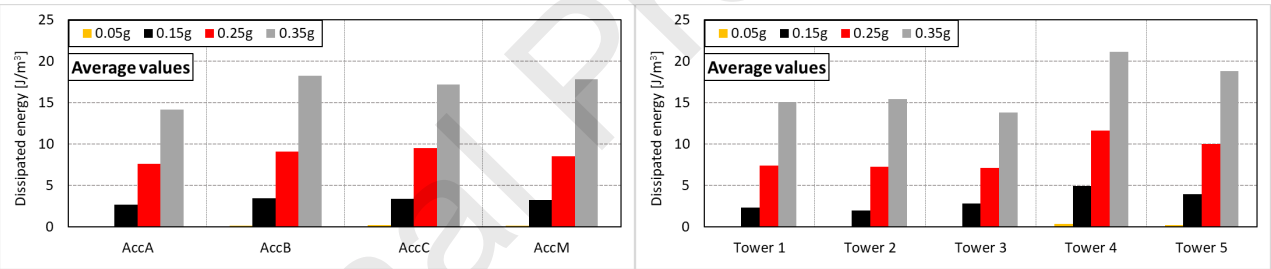

Fig. 23. Average values of the energy density dissipated by tensile damage (EDDTD) registered for the four accelerograms (left) and for the five bell towers (right) at the end of the non-linear dynamic analyses with different PGA values.

Fig. 24 shows the average values of the energy density dissipated by tensile damage (EDDTD) in the five parts of the bell towers for the four accelerograms and for the five case studies at the end of the non-linear dynamic analyses with PGA=0.15g and PGA=0.35g.

-A similar EDDTD distribution among the five parts of each bell tower can be observed for the different accelerograms. In particular, the belfry (Level 4) presents the highest EDDTD values for all the accelerograms, under both PGA=0.15g and PGA=0.35g: moreover, high EDDTD values are registered also for Level 3 for all the accelerograms, especially under PGA=0.35g. It can be noted that the difference of EDDTD values between Level 3 and Level 4 decreases when PGA increases: in fact, as observed from the damage contour plots, extensive damage spreads below the belfry under high PGA values. On the other hand, it is important to point out that the EDDTD values registered at Level 1 and Level 2 are lower for AccA than for the other accelerograms.

-Among the different bell towers, Tower 5 presents the highest EDDTD values in the middle-upper parts (Levels 3-4-5), which are characterized by large openings and remarkable reductions of walls thickness.

-Tower 4 presents the most uniform distribution of damage in Levels 2-5 among the different bell towers. Due to the reduced values of the walls thickness (30-40 cm) along the whole height of the

bell tower, the noticeable damage initially generated in the belfry propagates easily in the lower parts of the structure. Moreover, it can be noted that the highest EDDTD values in the bottom parts (Levels 1-2) are observed for Tower 4 and Tower 2 because of the reduced base walls thickness.
-A similar damage distribution can be observed for Tower 1, Tower 2 and Tower 3, which present a recurrent significant damage concentration in Levels 3-4 under PGA=0.35g and a remarkable damage increase in the bottom part (Level 1) passing from PGA=0.15g to PGA=0.35g.

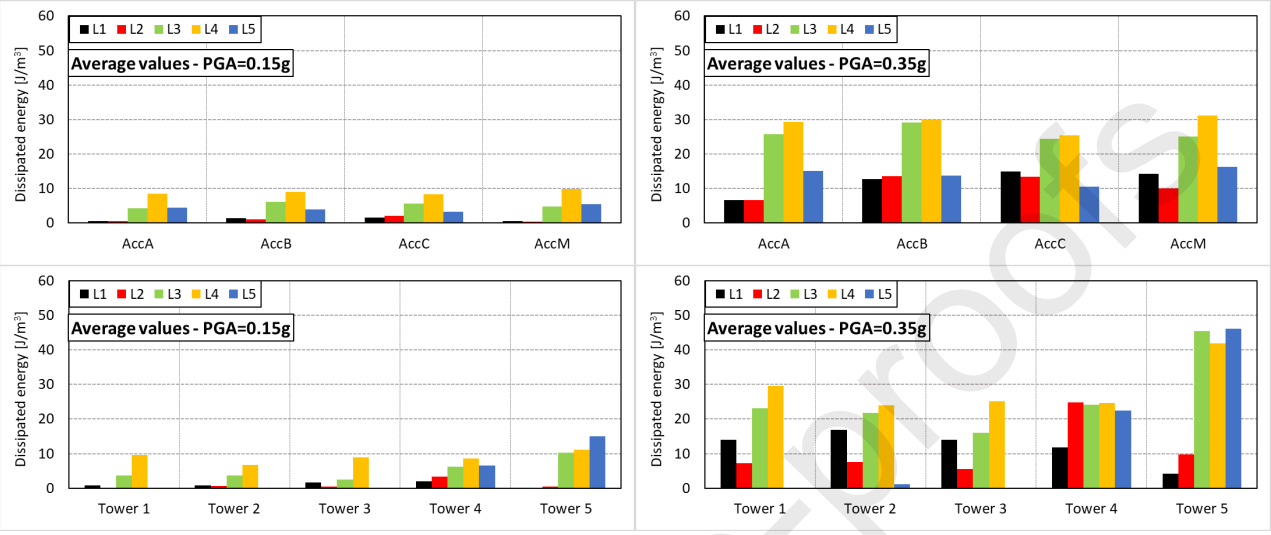

Fig. 24. Average values of the energy density dissipated by tensile damage (EDDTD) registered in the five parts of the bell towers for the four accelerograms (top) and for the five bell towers (bottom) at the end of the non-linear dynamic analyses with PGA=0.15g and PGA=0.35g.

6.4. Simplified approach and non-linear dynamic analysis

A comparison of the results obtained through the simplified approach proposed by the Italian Code and the non-linear dynamic analyses is carried out for different seismic intensity levels.
-For smaller seismic intensity levels (Sa_g=0.05g), the seismic safety Index computed according to the simplified method is larger than one for all the bell towers considering the different ground types. The non-linear dynamic analyses show very limited damage patterns, with recurrent damage concentrations near the large openings of the belfry and some small horizontal cracks at the base. Such a result obtained from the non-linear dynamic analyses allows identifying the potential structural weakness zones of the bell tower from which damage may propagate for higher PGA values.
-For medium seismic intensity levels (Sa_g=0.15g), the seismic safety Index computed according to the simplified method is smaller than one at the base of the majority of the bell towers, especially in correspondence with openings. The non-linear dynamic analyses show more extensive damage patterns in the upper part and at the base of the bell towers.
-For higher seismic intensity levels (Sa_g=0.25g and Sa_g=0.35g), the seismic safety Index computed according to the simplified method is smaller than one at the base of all the bell towers and in correspondence with the belfry of the majority of the bell towers. The non-linear dynamic analyses show severe damage patterns in the upper part and at the base of the bell towers, along with very widespread damage distributions along the height.
-From the analyses of the results, it can be stated that the simplified method may provide a preliminary conservative global assessment of the seismic safety of the structure, but it is not able to accurately identify the structural weaknesses and seismic vulnerability of all the different parts of the bell tower.
-The simplified method indicates the bottom part of the bell tower as the potential critical region, which is subjected to high gravity loads and exhibits a reduced resisting bending moment in correspondence with openings. The seismic safety Index is smaller than one for intermediate seismic

intensity levels (Sa_g=0.15g) for the majority of the bell towers. Conversely, the non-linear dynamic analyses show severe damage concentrations mainly in the upper parts of the bell towers, which are characterized by large openings and reduced walls thickness: for high PGA values, widespread damage is observed also along the whole height of the bell tower. Such a discrepancy can be clearly observed for Tower 5. The simplified method indicates that the base section is the most vulnerable part, while the non-linear dynamic analyses show damage concentrations in the middle and upper parts of the bell tower, presenting large openings and remarkable reductions of walls thickness. On the contrary, damage patterns at the base are limited due to the largest section sizes and walls thickness.

-Other two relevant discrepancies between the results of the simplified method and the non-linear dynamic analyses can be observed in the case of Tower 4 and Tower 3.

-According to the simplified method, Tower 4 presents the highest seismic safety Index due to the smallest weight and the lowest height among all the bell towers. In addition, the bell tower is also characterized by large base section sides providing high values of resisting bending moment. On the contrary, the non-linear dynamic analyses highlight that Tower 4 presents the highest EDDTD values: this result is mainly related to the small values of the walls thickness. The damage originated near the openings of the upper part propagates along the whole height of the bell tower.

-According to the simplified method, Tower 3 presents the lowest seismic safety Index. Such a result can be mainly attributed to the resisting bending moment reduction of the critical base section due to the presence of openings in both the directions: moreover, the dimensions of the critical base section sides are the smallest among the bell towers. On the contrary, the non-linear dynamic analyses show that Tower 3 presents the lowest EDDTD values. Such a result is mainly due to the regular thickness of the walls along the height and the absence of openings in the central part of the tower.

7. Conclusions

This study has provided a comprehensive insight into the seismic vulnerability and earthquake response of five slender historical masonry bell towers through a simplified approach suggested by the Italian Code and advanced numerical simulations. The five case studies investigated in this work represent a common structural typology that is widespread in South-East Lombardia, Northern Italy. For the non-linear dynamic analyses, detailed FE models of the bell towers have been developed and a damage plasticity behavior exhibiting softening in both tension and compression has been adopted for masonry.

The following observations and remarks can be made from the analyses carried out in this study.

-A careful examination of the results indicates that the simplified procedure may provide reasonable synthetic predictions only for a fast preliminary assessment of the seismic vulnerability of the bell towers. It can be noted that the simplified procedure is generally more conservative than the non-linear dynamic analyses: such a result is partially due to the assumption that tensile resistance is neglected for masonry within the simplified approach. Moreover, the simplified approach is not able to accurately identify the real structural weaknesses of the different parts of the bell towers, especially the high seismic vulnerability of the belfry.

-The results of the non-linear dynamic analyses show that the seismic response of the bell towers is affected by both the main geometrical features of the structure and the spectral accelerations correlated to the main vibration modes. High slenderness, presence of large openings, small walls thickness and reduced base sections make the bell towers particularly vulnerable to seismic actions, especially in cases where the related vibration modes with considerable participating mass ratio correspond to high amplifications of the spectral acceleration.

-The evaluation of the maximum normalized displacements obtained from the non-linear dynamic analyses highlights the relevant influence of the accelerograms characteristics. A significant difference of normalized top displacements is observed for the different accelerograms used in this

study: in particular, the largest normalized displacements are registered for AccM and the smallest ones are registered for AccA. On the other hand, similar values (within the range 0.6%-0.8% under PGA=0.35g) of normalized top displacements are obtained for the different bell towers. Moreover, it is important to point out the effects of the different characteristics of the two orthogonal components of an accelerogram. For all the bell towers, the largest normalized displacements are registered in the Y direction under the application of AccM, which means that the north-south (Y direction) accelerogram component is more severe than the east-west (X direction) one.

-A clear influence of the accelerograms characteristics can be also observed for the EDDTD values registered at the end of the non-linear dynamic analyses: significantly lower EDDTD values are computed in the case of AccA. On the other hand, the accelerograms characteristics have minor influence on damage patterns and EDDTD distributions: in such cases, the geometrical features of the bell towers appear to play a more important role than the accelerograms characteristics.

-The highest EDDTD values are registered in the upper parts (Level 4 and Level 3) of the bell towers for all the accelerograms. The belfry (Level 4) shows significant damage even for small-to-moderate seismic intensity levels, while the part below the belfry (Level 3) suffers widespread damage, especially for high PGA values. The dome (Level 5) generally presents negligible damage, except for Tower 4 and Tower 5.

-The examination of tensile damage contour plots shows that the first visible cracks are concentrated near the large openings of the upper part and at the base of the bell towers, even for small PGA values. Increasing the PGA values, damage is generally distributed throughout the different parts of the bell towers, especially in presence of reduced walls thickness. A remarkable damage concentration due to vertical irregularities can be detected in correspondence with sharp reductions of the sections along the height of the bell towers.

-Large normalized displacements are generally correlated to high EDDTD values, especially in the case of extensive damage and global collapse of the bell tower. However, in some cases, a clear correlation between maximum normalized displacements and EDDTD values does not clearly emerge, especially in the case of concentrated damage and collapse mechanisms involving only a specific part of the bell tower.

References

[1] Lagomarsino S. Damage assessment of churches after L'Aquila earthquake (2009). Bulletin of Earthquake Engineering 2012;10(1):73-92.

[2] Grillanda N, Valente M, Milani G, Chiozzi A, Tralli A. Advanced numerical strategies for seismic assessment of historical masonry aggregates. Engineering Structures 2020;212:article 110441.

[3] Habieb AB, Valente M, Milani G. Hybrid seismic base isolation of a historical masonry church using unbonded fiber reinforced elastomeric isolators and shape memory alloy wires. Engineering Structures 2019;196: 109281.

[4] Mosoarca M, Onescu I, Onescu E, Anastasiadis A. Seismic vulnerability assessment methodology for historic masonry buildings in the near-field areas. Engineering Failure Analysis 2020, 104662.

[5] Silva LC, Mendes N, Lourenço PB, Ingham J. Seismic Structural Assessment of the Christchurch Catholic Basilica, New Zealand. Structures 2018;15:115-130.

[6] Casolo S, Uva, G. Nonlinear analysis of out-of-plane masonry façades: full dynamic versus pushover methods by rigid body and spring model. Earthquake Engineering & Structural Dynamics 2013;2(4):499-521.

[7] Hofer L, Zampieri P, Zanini MA, Faleschini F, Pellegrino C. Seismic damage survey and empirical fragility curves for churches after the August 24, 2016 Central Italy earthquake. Soil Dynamics and Earthquake Engineering 2018;111:98-109.

[8] Gattulli V, Antonacci E, Vestroni F. Field observations and failure analysis of the Basilica S. Maria di Collemaggio after the 2009 L'Aquila earthquake. Engineering Failure Analysis 2013;34:715-734.

[9] Crespi P, Franchi A, Giordano N, Scamardo M, Ronca P. Structural analysis of stone masonry columns of the Basilica S. Maria di Collemaggio. Engineering Structures 2016;129:81-90.
[10] Barbieri G, Valente M, Biolzi L, Togliani C, Fregonese L, Stanga G. An insight in the late Baroque architecture: an integrated approach for a unique Bibiena church. Journal of Cultural Heritage 2017;23:58-67.
[11] Vlachakis G, Vlachaki E, Lourenço PB. Learning from failure: Damage and failure of masonry structures, after the 2017 Lesvos earthquake (Greece). Engineering Failure Analysis 2020;117: 104803.
[12] Genç AF, Ergün M, Günaydin M, Altunişik AC, Ateş Ş, Okur FY, Mosallam AS. Dynamic analyses of experimentally-updated FE model of historical masonry clock towers using site-specific seismic characteristics and scaling parameters according to the 2018 Turkey building earthquake code. Engineering Failure Analysis 2019;105:402-426.
[13] Bayraktar A, CoŞkun N, Yalçin A. Damages of masonry buildings during the July 2, 2004 Doğubayazıt (Ağrı) earthquake in Turkey. Engineering Failure Analysis 2007;14(1):147-157.
[14] Shakya M, Kawan CK, Gaire AK, Duwal S. Post-earthquake damage assessment of traditional masonry buildings: A case study of Bhaktapur municipality following 2015 Gorkha (Nepal) earthquake. Engineering Failure Analysis 2021;123:105277.
[15] Sarhosis V, Milani G, Formisano A, Fabbrocino F. Evaluation of different approaches for the estimation of the seismic vulnerability of masonry towers. Bulletin of Earthquake Engineering 2018;16(3):1511-1545.
[16] Habieb AB, Valente M, Milani G. Effectiveness of different base isolation systems for seismic protection: numerical insights into an existing masonry bell tower. Soil Dynamics and Earthquake Engineering 2019;125, article 105752.
[17] Casolo S. A three-dimensional model for vulnerability analysis of slender medieval masonry towers. Journal of Earthquake Engineering 1998;2(04):487-512.
[18] Casolo S, Milani G, Uva G, Alessandri C. Comparative seismic vulnerability analysis on ten masonry towers in the coastal Po Valley in Italy. Engineering Structures 2013:49;465-490.
[19] Casolo S, Diana V, Uva G. Influence of soil deformability on the seismic response of a masonry tower. Bulletin of Earthquake Engineering 2017;15(5):1991-2014.
[20] Preciado A, Bartoli G, Ramírez-Gaytán A. Earthquake protection of the Torre Grossa medieval tower of San Gimignano, Italy by vertical external prestressing. Engineering Failure Analysis 2017;71:31-42.
[21] Preciado A, Sperbeck ST, Ramírez-Gaytán A. Seismic vulnerability enhancement of medieval and masonry bell towers externally prestressed with unbonded smart tendons. Engineering Structures 2016;122:50-61.
[22] Preciado A, Santos JC, Silva C, Ramírez-Gaytán A, Falcon JM. Seismic damage and retrofitting identification in unreinforced masonry Churches and bell towers by the september 19, 2017 (Mw= 7.1) Puebla-Morelos earthquake. Engineering Failure Analysis 2020;118:104924.
[23] Preciado A. Seismic vulnerability and failure modes simulation of ancient masonry towers by validated virtual finite element models. Engineering Failure Analysis 2015;57:72-87.
[24] Erdogan YS, Kocatürk T, Demir C. Investigation of the seismic behavior of a historical masonry minaret considering the interaction with surrounding structures. Journal of Earthquake Engineering 2019;23(1):112-140.
[25] Kocaturk T, Erdogan YS. Earthquake behavior of M1 minaret of historical sultan ahmed mosque (blue mosque). Structural Engineering and Mechanics 2016;59(3):539-558.
[26] Bayraktar A, Hökelekli E, Halifeoğlu FM, Mosallam A, Karadeniz H. Vertical strong ground motion effects on seismic damage propagations of historical masonry rectangular minarets. Engineering Failure Analysis 2018;91:115-128.
[27] Bayraktar A, Hökelekli E. A cost-effective FRCM technique for seismic strengthening of minarets. Engineering Structures 2021, 229, 111672.

[28] Bayraktar A, Altunişik AC, Sevim B, Türker T. Seismic response of a historical masonry minaret using a finite element model updated with operational modal testing. Journal of Vibration and Control 2011;17(1):129-149.
[29] Bartoli G, Betti M, Galano L, Zini G. Numerical insights on the seismic risk of confined masonry towers. Engineering Structures 2019;180:713-727.
[30] Bartoli G, Betti M, Monchetti S. Seismic risk assessment of historic masonry towers: comparison of four case studies. Journal of Performance of Constructed Facilities 2017;31(5): 04017039.
[31] Torelli G, D'Ayala D, Betti M, Bartoli G. Analytical and numerical seismic assessment of heritage masonry towers. Bulletin of Earthquake Engineering 2020;18(3):969-1008.
[32] Ferraioli M, Lavino A, Abruzzese D, Avossa AM. Seismic assessment, repair and strengthening of a medieval masonry tower in southern Italy. International Journal of Civil Engineering 2020;18(9):967-994.
[33] Bartoli G, Betti M, Vignoli A. A numerical study on seismic risk assessment of historic masonry towers: a case study in San Gimignano. Bulletin of Earthquake Engineering 2016;14(6):1475-1518.
[34] Micelli F, Cascardi A. Structural assessment and seismic analysis of a 14th century masonry tower. Engineering Failure Analysis 2020;107:104198.
[35] Pineda P. Collapse and upgrading mechanisms associated to the structural materials of a deteriorated masonry tower. Nonlinear assessment under different damage and loading levels. Engineering Failure Analysis 2016;63:72-93.
[36] Bayraktar A, Şahin A, Özcan DM, Yildirim F. Numerical damage assessment of Haghia Sophia bell tower by nonlinear FE modeling. Applied Mathematical Modelling 2010;34(1):92-121.
[37] DM 14/01/2008. Nuove norme tecniche per le costruzioni. Ministero delle Infrastrutture (GU n.29 04/02/2008), Rome, Italy. [New technical norms on constructions].
[38] Circolare n° 617 del 2 febbraio 2009. Istruzioni per l'applicazione delle nuove norme tecniche per le costruzioni di cui al decreto ministeriale 14 gennaio 2008. [Instructions for the application of the new technical norms on constructions].
[39] DPCM 9/2/2011. Linee guida per la valutazione e la riduzione del rischio sismico del patrimonio culturale con riferimento alle Norme tecniche delle costruzioni di cui al decreto del Ministero delle Infrastrutture e dei trasporti del 14 gennaio 2008. [Italian guidelines for the evaluation and the reduction of the seismic risk for the built heritage, with reference to the Italian norm of constructions].
[40] Eurocode 8. Design provisions for earthquake resistance of structures. Part 1: General rules - seismic actions and general requirements for structures, European Committee for Standardization, Brussels, Belgium, 2004.
[41] ABAQUS®, Theory Manual, Version 6.14.
[42] Valente M, Milani G. Advanced numerical insights into failure analysis and strengthening of monumental masonry churches under seismic actions. Engineering Failure Analysis 2019;103: 410-430.
[43] Valente M, Milani G. Earthquake-induced damage assessment and partial failure mechanisms of an Italian Medieval castle. Engineering Failure Analysis 2019;99:292-309.
[44] Bartoli G, Betti M, Marra AM, Monchetti S. Semiempirical formulations for estimating the main frequency of slender masonry towers. Journal of Performance of Constructed Facilities 2017; 31(4): article 04017025.
[45] Diaferio M, Foti D, Potenza F. Prediction of the fundamental frequencies and modal shapes of historic masonry towers by empirical equations based on experimental data. Engineering Structures 2018;156:433-442.
[46] Shakya M, Varum H, Vicente R, Costa A. Empirical formulation for estimating the fundamental frequency of slender masonry structures, Int. J. Archit. Heritage 2016; 10(1):55-66.
[47] Bayraktar A, Çalik I, Türker T. A Simplified Fundamental Frequency Formulation Based on In-Situ Tests for Masonry Stone Minarets. Experimental Techniques 2021, 1-14.

[48] Vanmarcke EH, Cornell CA, Gasparini DA, Hou S. SIMQKE: a program for artificial motion generation. Massachusetts: Civil Engineering Department, Massachusetts Institute of Technology; 1976.

Highlights

- seismic assessment and earthquake response of slender historical masonry bell towers
- seismic response is affected by the main geometrical features and main vibration properties of the bell towers
- damage distribution among the different parts of the bell towers for different PGA values
- influence of different accelerograms on the energy density dissipated by tensile damage and maximum top displacements
- main limitations of the simplified approach are highlighted through a comparison with non-linear dynamic analyses

Declaration of interests

☒ The authors declare that they have no known competing financial interests or personal relationships that could have appeared to influence the work reported in this paper.

☐ The authors declare the following financial interests/personal relationships which may be considered as potential competing interests: